EUROPEAN JOURNAL OF PURE AND APPLIED MATHEMATICS
2025, Vol. 18, Issue 2, Article Number 5913
ISSN 1307-5543 – ejpam.com
Published by New York Business Global

Impact of Singular and Non-Singular Kernels on Crossover Monkeypox Mathematical Model

N. H. Sweilam[1,*], S. M. Al-Mekhlafi[2,3], A. Ahmed[4], D. G. Mohamed[4], E. M. Abo-Eldahab[4]

[1] *Mathematics Department, Faculty of Science, Cairo University, Giza, Egypt*
[2] *Mathematics Department, Faculty of Education, Sana'a University, Yemen*
[3] *Department of Engineering Mathematics and Physics, Future University in Egypt, Egypt*
[4] *Mathematics Department, Faculty of Science, Helwan University, Cairo, Egypt*

Abstract. This study presents three crossover models describing monkeypox disease that includes Caputo, Mittag-Leffler, and Caputo-Fabrizio definitions. To represent the monkeypox disease, three models of variable-order fractional, fractal-fractional, and stochastic, as well as their piecewise derivatives are provided at three different time periods. To approximate these models, we use the nonstandard Grünwald-Letnikov finite difference method to approximate the deterministic model with a singular kernel and a nonsingular Mittag-Leffler kernel to approximate the deterministic model using the Toufik-Atangana method. Moreover, we use the approximation of the integral Caputo-Fabrizio and Lagrange polynomial of two steps to approximate the deterministic model with a nonsingular exponential decay kernel. We implemented the Milstein method to approximate the stochastic differential equation. An analysis of the suggested model's stability is conducted. The effectiveness of the procedures was confirmed, and the theoretical results were supported through numerical testing and comparisons with actual data.

2020 Mathematics Subject Classifications: 65L05, 26A33, 39A50

Key Words and Phrases: Monkeypox disease, fractal-fractional derivative, Milstein method, Atangana-Baleanu Caputo operator, Caputo-Fabrizio operator

1. Introduction

The Monkeypox virus is the cause of this uncommon viral zoonotic disease. Monkeypox, first identified in 1958, is a pox-like disease caused by the virus known as variola. It leads to fever, rash, and lymphadenopathy, with severe cases in children, pregnant women,

*Corresponding author.
DOI: https://doi.org/10.29020/nybg.ejpam.v18i2.5913

Email addresses: nsweilam@sci.cu.edu.eg (N. H. Sweilam), sih.almikhlafi@su.edu.ye (S. M. Al-Mekhlafi), aya.a.mahmoud@science.helwan.edu.eg (A. Ahmed), doaa.gamal@science.helwan.edu.eg (D. G. Mohamed), emad.aboeldahab@yahoo.com (E. M. Abo-Eldahab)

and immunocompromised individuals. Monkeypox cases have been reported in central and western African nations before the 2022 outbreak, with most cases linked to travel to endemic countries [1]. Since May 2022, cases have been found in non-endemic and endemic countries, with most cases recorded in sexual health services. The biology, spread, threat, vaccinations, and available therapies of the virus are examined [2]. Researchers have suggested a number of theoretical and mathematical investigations to examine the dynamics of monkeypox [3], including analyzing its ecological niche, geographic distribution, projected burden, and transmission dynamics [4]. They have also proposed models for treatment and vaccination [5], a stochastic model [6], A new model that takes into account transfer from person to person [7], and a game-theoretic model for assessing vaccination plans [8].

Fractional calculus is being increasingly applied in science and engineering, particularly in modeling deathly epidemics [6]. Recent works have focused on optimal control problems [9], two-strain epidemic models [10], and there are numerous models using various fractional derivatives [11]. This trend is gaining traction in various fields. Researchers have developed various models for various diseases, including Covid-19, vaccination efficacy, cholera outbreaks, human African trypanosomiasis epidemics, hepatitis B virus, and dengue fever and zika virus coinfection [12]-[13]. Also, there are important applications of Atangana-Baleanu, Caputo-Fabrizo, Caputo derivatives can be found in [14], [15], [16].

These models use integer and fractional derivatives, fractional derivatives, and mathematical techniques to analyze and control various diseases. Epidemiology modelling is intended to benefit from the use of generalised fractional mathematical models. Its main advantages include improved data fitting, multistage, capturing factuality and memory effects. A powerful tool for taking into consideration the system's memory and inherited traits is provided by fractional epidemic models, as opposed to integer-order derivative for models which either disregard or prevent this from occurred. Furthermore, in terms of data fitting, the fractional variant provides one extra degree of flexibility over the integer model. A fractional system has various benefits, including the opportunity to select the fractional ordered value that best describes a model in practice, memory, and the most precise data fitting. The fractional derivatives models are further reinforced by inherited traits, making them more appropriate for representing real-world phenomena [17, 18].

In order to better represent the complex behaviours of certain real-world situations, piecewise calculus has been developed in recent years. Various real-world phenomena, such as infectious illnesses, heat transport, fluid dynamics, and intricate advection issues, exhibit crossover behaviours [19]. Interestingly, recent studies indicate that piecewise formulations in differential equations give a more realistic depiction of these processes than standard fractional order or integer order methods. Remarkably, the notions of piecewise derivatives and short memory in fractional calculus are very similar. Considerable recent work has been done in this area, including citations to important publications like [20].

Our motivation stems from the complex and heterogeneous nature of infectious disease dynamics, where traditional integer-order models may not fully capture the underlying memory effects, spatial heterogeneity, and randomness in disease transmission.

- Variable-order fractional derivatives allow us to incorporate time-dependent changes in disease progression, reflecting evolving immunity, interventions, and behavioral adapta-

tions.
- Fractal-fractional derivatives help model spatial heterogeneity and self-similar transmission patterns, which are particularly relevant in disease spread across different community structures.
- Stochastic derivatives account for randomness in infection rates, environmental variations, and uncertainties in disease reporting, making the model more realistic in capturing real-world epidemic fluctuations.
These advanced modeling techniques offer a more flexible and accurate framework compared to traditional approaches, ultimately improving predictive power and decision-making in epidemiological studies.

In order to create three new crossover systems for the Monkypox model, which is introduced for the first time in this paper, with the variable-order and fractal-fractional derivatives defined by three definitions (Atangana-Baleanu, Caputo-Fabrizo, and Caputo derivatives), we will apply stochastic derivatives to piecewise differential equations. The stability analysis of the fundamental system will be covered. Furthermore, we will investigate the behaviour of stochastic derivatives using the Milstein technique and solve a crossover model based on a non-singular kernel described by Atangana-Baleanu derivatives using Toufik-Atangana method (TAM). Additionally, we employ the approximation of integral Caputo-Fabrizio and Lagrange polynomial of two steps to approximate the deterministic model with a nonsingular exponential decay kernel. We will use the Grünwald−Letnikov nonstandard finite difference technique (GL-NSFDM) to approximate a determinate model utilising a singular kernel. The outcomes of infected persons derived from the suggested models are contrasted with actual data, whereby the US monkeypox data (June 13-September 16, 2022). Furthermore, A comparison between the three methods with the Milstein method for solving the three crossover models is presented. A number of numerical simulations utilising variable order and fractional orders will be shown.

The following is the study's structure: pertinent definitions of fractional and variable-order Caputo derivatives are given in Section 2. Also, a brief overview of stochastic equations and a numerical method for solving them was presented in this section. Section 3 presents three distinct generalised crossover mathematical models for the monkeypox virus based on principles of variable, fractal-fractional order, and the notions stochastic in three intervals; these crossover mathematical models defined by Atangana-Baleanu, Caputo-Fabrizo, Caputo derivatives. Section 4 theoretical analysis of basic model is examined. Section 5 illustrates constructing GL-NSFDM to approximate the deterministic model using a singular kernel and the TAM, which uses a nonsingular Mittag-Leffler kernel to approximate the deterministic model. Moreover, Utilising the approximation of integral Caputo-Fabrizio and Lagrange polynomial of two steps to approximate the deterministic model with a nonsingular exponential decay kernel. Numerical simulations of the three suggested models are shown in Section 5. Lastly, a summary of the study's main conclusions and contributions is given in Section 6.

2. Fundamental Definitions

We provide a few key definitions for fractional that will be utilised in the rest of this research in the section that follows.

Definition 2.1. *The derivatives of order α of Caputo's for $f(t)$ are determined by [9]:*

$$ {}_0^C D_t^{\alpha}(f(t)) = \frac{1}{\Gamma(n-\alpha)} \int_0^t (t-s)^{n-\alpha-1} f^{(n)}(s) ds, \quad t > 0, \tag{1} $$

where $n = \mathbb{N}$, $n-1 < \alpha \leq n$, and $\Gamma(\cdot)$ is a Gamma function.

Definition 2.2. *The Caputo fractal-fractional derivative of a function $f(t)$ is defined by fractal order β and fractional order α and a power law kernel as follows [9]:*

$$ {}_0^{FFC} D_t^{\alpha,\beta}(f(t)) = \frac{1}{\Gamma(n-\alpha)} \int_0^t (t-s)^{n-\alpha-1} (\frac{d}{ds^{\beta}} f(s)) ds, \tag{2} $$

where $(n-1) < \alpha$, $\beta \leq n \in \mathbb{N}$.

Definition 2.3. *(Atangana - Baleanu Caputo fractional derivative)[21]*

$$ {}_a^{ABC} D_t^{\alpha}(f(t)) = \frac{AB(\alpha)}{1-\alpha} \int_a^t f'(s) E_{\alpha}(-\alpha \frac{(t-s)^{\alpha}}{1-\alpha}) ds, \tag{3} $$

$\alpha \in [0,1]$, $AB(\alpha) = 1-\alpha+\frac{\alpha}{\Gamma(\alpha)}$ and the Mittag Leffler function is an entire function defined by
$E_{\alpha}(z) = \sum_{k=0}^{\infty} \frac{z^k}{\Gamma(k\alpha+1)}$.

Definition 2.4. *The fractal-fractional derivative of $f(t)$ with the Mittag-Leffler type kernel and an order of α, may be found by [22].*

$$ {}_0^{FFAB} D_t^{\alpha,\beta}(f(t)) = \frac{AB(\alpha)}{(1-\alpha)} \int_0^t \frac{d}{dt^{\beta}} f(s) E_{\alpha}(-\alpha \frac{(t-s)^{\alpha}}{1-\alpha}) ds, \tag{4} $$

such that: $\alpha \in [0,1]$, $AB(\alpha) = 1-\alpha+\frac{\alpha}{\Gamma(\alpha)}$ and $E_{\alpha}(z) = \sum_{k=0}^{\infty} \frac{z^k}{\Gamma(k\alpha+1)}$ characterises the Mittag Leffler function.

Definition 2.5. *The form of Atangana - Baleanu fractal-fractional integral is [21]*

$$ {}_0^{FFAB} I_t^{\alpha,\beta}(f(t)) = \frac{\alpha\beta}{AB(\alpha)\Gamma(\alpha)} \int_0^t f(s)(t-s)^{\alpha-1} s^{\beta-1} ds + \frac{1-\alpha}{AB(\alpha)} \beta t^{\beta-1} f(t), \tag{5} $$

here $\alpha \in [0,1]$, $AB(\alpha) = 1-\alpha+\frac{\alpha}{\Gamma(\alpha)}$ and $E_{\alpha}(z) = \sum_{k=0}^{\infty} \frac{z^k}{\Gamma(k\alpha+1)}$ characterises the Mittag Leffler function.

Definition 2.6. *The definition of the Caputo-Fabrizio fractional derivative[15].*

$$ {}_0^{CF}D_t^{\alpha}(f(t)) = \frac{M(\alpha)}{1-\alpha}\int_0^t \frac{d}{ds}f(s)e^{(\frac{-\alpha}{1-\alpha}(t-s))}ds, \tag{6}$$

Consider α to be a fractional order constant with the value $0 < \alpha \leq 1$ and $M(\alpha) = 1-\alpha+\frac{\alpha}{\Gamma(\alpha)}$.

Definition 2.7. *The fractional integral of the function f(t) with an exponential decay kernel is provided by [21]*

$$ {}_0^{CF}I_t^{\alpha}(f(t)) = \frac{\alpha}{M(\alpha)}\int_0^t f(s)ds + \frac{1}{M(\alpha)}(1-\alpha)f(t), \tag{7}$$

In this case, $M(\alpha)$ represents a normalising function, $M(0) = 1, M(1) = 1$ and $0 < \alpha \leq 1$.

Definition 2.8. *The Caputo-Fabrizio fractal-fractional derivative[22].*

$$ {}_0^{FFCF}D_t^{\alpha,\beta}(f(t)) = \frac{M(\alpha)}{1-\alpha}\frac{d}{dt^{\beta}}\int_0^t \exp(-\frac{\alpha}{1-\alpha}(t-s))f(s)ds, \tag{8}$$

whereas $M(0) = M(1) = 1$, $0 < \alpha \leq 1$, and $\beta \leq n \in \mathbb{N}$.

Definition 2.9. *With order α and an exponentially decaying type kernel, the fractal-fractional integral of $f(t)$ is provided by [21].*

$$ {}_0^{FFCF}I_t^{\alpha,\beta}(f(t)) = \frac{\alpha\beta}{M(\alpha)}\int_0^t s^{\beta-1}f(s)ds + \frac{\beta(1-\alpha)t^{\beta-1}f(t)}{M(\alpha)}, \tag{9}$$

In this case, $M(\alpha)$ represents a normalising function, $M(0) = 1, M(1) = 1$ and $0 < \alpha \leq 1$.

2.1. Stochastic Differential Equation (SDE)

Consider the real-valued process $Y(t)$ with $t \in [0, T]$ satisfying the following a stochastic differential equation (SDE) [23].

$$ dY(t) = \Phi(Y(t), t)dt + \sigma\Psi(Y(t), t)\Delta B(t), \tag{10}$$

where $\Delta B = B(t_{n+1}) - B(t_n)$ is the Brownian increment on $[t_n, t_{n+1}]$.

2.2. Milstein method

By including a second-order "correction" factor, which is obtained from the stochastic Taylor series expansion of $Y(t)$ by using Ito's lemma on the $\Phi(.)$ and $\Psi(.)$ functions, Milstein technique improves the accuracy of the Euler-Maruyama method approximation. The following differential form is obtained using the Milstein technique [24]:

$$ Y_{n+1} - Y_n = \Phi(Y_n, t_n)h + \Psi(Y_n, t_n)\Delta B_n + 0.5\Psi'(Y_n, t_n)\Psi(Y_n, t_n)((\Delta B_n)^2 - h), \tag{11}$$

where $\Psi'(Y(t), t)$ denotes the derivative of $\Psi(Y(t), t)$, $\Delta B = B(t_{n+1}) - B(t_n)$ is the Brownian increment on $[t_n, t_{n+1}]$.

3. The Crossover of Monkeypox Mathematical Model

Here we modified the analysis of monkeypox virus using mathematics which given in [25] to a hybrid piecewise variable of fractional, fractal-fractional order, and stochastic Monkeypox disease mathematical model. Using the idea of a system of piecewise differential equations, we will present three models; two models with nonsingular kernel and the third one with singular kernel. The impact of singular and non-singular kernels on the crossover monkeypox mathematical model primarily affects how the memory and hereditary effects are incorporated into the model. Singular and non-singular kernels arise in fractional-order differential equations, which are increasingly used to model infectious diseases due to their ability to capture long-term memory effects.

3.1. The Crossover of Monkeypox Mathematical Model with Nonsingular Kernel (CM1)

A crossover monkeypox model considers both human-to-human and animal-to-human transmission pathways. The choice of kernel affects:

- Epidemic Threshold (Basic Reproduction Number, R_0): Singular kernels might lead to higher R_0 due to stronger memory effects, whereas non-singular kernels may predict lower, more immediate transmission dynamics.
- Peak Infection Time: Singular kernels delay the infection peak, while non-singular kernels lead to a more immediate peak.

Applying the Atangana–Baleanu definition , it incorporates a nonsingular and nonlocal kernel, making it suitable for modeling memory effects in complex systems. Also, it gives rise to the idea of a piecewise system of differential equations. The Atangana–Baleanu variable order operator 'κ' is used to extend the deterministic model in $0 < t \leq t_1$, the fractal-fractional of the Atangana–Baleanu is employed in $t_1 < t \leq t_2$, and the stochastic differential equation (SDE) in $t_2 < t \leq T_f$. The following is an expression of the new model:

$$
\begin{aligned}
{}_0^{ABC}D_t^{\kappa} S_h &= \Lambda_h^{\kappa} - \frac{(\beta_1^{\kappa} I_r + \beta_2^{\kappa} I_h) S_h}{N_h} - \mu_h^{\kappa} S_h + \phi^{\kappa} Q_h, \\
{}_0^{ABC}D_t^{\kappa} E_h &= \frac{(\beta_1^{\kappa} I_r + \beta_2^{\kappa} I_h) S_h}{N_h} - (\gamma_1^{\kappa} + \gamma_2^{\kappa} + \mu_h^{\kappa}) E_h, \\
{}_0^{ABC}D_t^{\kappa} I_h &= \gamma_1^{\kappa} E_h - (\mu_h^{\kappa} + \delta_h^{\kappa} + \rho^{\kappa}) I_h, \\
{}_0^{ABC}D_t^{\kappa} Q_h &= \gamma_2^{\kappa} E_h - (\phi^{\kappa} + \tau^{\kappa} + \mu_h^{\kappa} + \delta_h^{\kappa}) Q_h, \\
{}_0^{ABC}D_t^{\kappa} R_h &= \rho^{\kappa} I_h + \tau^{\kappa} Q_h - \mu_h^{\kappa} R_h, \\
{}_0^{ABC}D_t^{\kappa} S_r &= \Lambda_r^{\kappa} - \frac{\beta_3^{\kappa} S_r I_r}{N_r} - \mu_r^{\kappa} S_r, \\
{}_0^{ABC}D_t^{\kappa} E_r &= \frac{\beta_3^{\kappa} S_r I_r}{N_r} - (\mu_r^{\kappa} + \gamma_3^{\kappa}) E_r,
\end{aligned}
$$

$$ {}_0^{ABC}D_t^{\kappa} I_r = \gamma_3^{\kappa} E_r - (\mu_r^{\kappa} + \delta_r^{\kappa}) I_r, \tag{12}$$

with initial conditions S_{h0}, E_{h0}, I_{h0}, Q_{h0}, R_{h0}, S_{r0}, E_{r0}, I_{r0} at $t = 0$. Furthermore, if $t_1 < t \leq t_2$, the model has the following expression:

$$\begin{aligned}
{}_0^{FFAB}D_t^{\alpha,\beta} S_h &= \Lambda_h^{\alpha} - \frac{(\beta_1^{\alpha} I_r + \beta_2^{\alpha} I_h) S_h}{N_h} - \mu_h^{\alpha} S_h + \phi^{\alpha} Q_h, \\
{}_0^{FFAB}D_t^{\alpha,\beta} E_h &= \frac{(\beta_1^{\alpha} I_r + \beta_2^{\alpha} I_h) S_h}{N_h} - (\gamma_1^{\alpha} + \gamma_2^{\alpha} + \mu_h^{\alpha}) E_h, \\
{}_0^{FFAB}D_t^{\alpha,\beta} I_h &= \gamma_1^{\alpha} E_h - (\mu_h^{\alpha} + \delta_h^{\alpha} + \rho^{\alpha}) I_h, \\
{}_0^{FFAB}D_t^{\alpha,\beta} Q_h &= \gamma_2^{\alpha} E_h - (\phi^{\alpha} + \tau^{\alpha} + \mu_h^{\alpha} + \delta_h^{\alpha}) Q_h, \\
{}_0^{FFAB}D_t^{\alpha,\beta} R_h &= \rho^{\alpha} I_h + \tau^{\alpha} Q_h - \mu_h^{\alpha} R_h, \\
{}_0^{FFAB}D_t^{\alpha,\beta} S_r &= \Lambda_r^{\alpha} - \frac{\beta_3^{\alpha} S_r I_r}{N_r} - \mu_r^{\alpha} S_r, \\
{}_0^{FFAB}D_t^{\alpha,\beta} E_r &= \frac{\beta_3^{\alpha} S_r I_r}{N_r} - (\mu_r^{\alpha} + \gamma_3^{\alpha}) E_r, \\
{}_0^{FFAB}D_t^{\alpha,\beta} I_r &= \gamma_3^{\alpha} E_r - (\mu_r^{\alpha} + \delta_r^{\alpha}) I_r,
\end{aligned} \tag{13}$$

with initial conditions

$$\begin{aligned}
&S_h(t_1) = S_{h1}, \quad E_h(t_1) = E_{h1}, \quad I_h(t_1) = I_{h1}, \quad S_r(t_1) = S_{r1}, \\
&R_h(t_1) = R_{h1}, \quad E_r(r_1) = E_{r1}, \quad Q_h(t_1) = Q_{h1}, \quad I_r(t_1) = I_{r1}.
\end{aligned}$$

Additionally, if $t_2 < t \leq T_f$, the model has the following expression:

$$\begin{aligned}
dS_h &= (\Lambda_h - \frac{(\beta_1 I_r + \beta_2 I_h) S_h}{N_h} - \mu_h S_h + \phi Q_h) dt + \sigma_1 S_h dB_1, \\
dE_h &= (\frac{(\beta_1 I_r + \beta_2 I_h) S_h}{N_h} - (\gamma_1 + \gamma_2 + \mu_h) E_h) dt + \sigma_2 E_h dB_2, \\
dI_h &= (\gamma_1 E_h - (\mu_h + \delta_h + \rho) I_h) dt + \sigma_3 I_h dB_3, \\
dQ_h &= (\gamma_2 E_h - (\phi + \tau + \mu_h + \delta_h) Q_h) dt + \sigma_4 Q_h dB_4, \\
dR_h &= (\rho I_h + \tau Q_h - \mu_h R_h) dt + \sigma_5 R_h dB_5, \\
dS_r &= (\Lambda_r - \frac{\beta_3 S_r I_r}{N_r} - \mu_r S_r) dt + \sigma_6 S_r dB_6, \\
dE_r &= (\frac{\beta_3 S_r I_r}{N_r} - (\mu_r + \gamma_3) E_r) dt + \sigma_7 E_r dB_7, \\
dI_r &= (\gamma_3 E_r - (\mu_r + \delta_r) I_r) dt + \sigma_8 I_r dB_8.
\end{aligned} \tag{14}$$

$$\begin{aligned}
&S_h(t_2) = S_{h2}, \quad E_h(t_2) = E_{h2}, \quad I_h(t_2) = I_{h2}, \quad Q_h(t_2) = Q_{h2}, \\
&R_h(t_2) = R_{h2}, \quad S_r(t_2) = S_{r2}, \quad E_r(r_2) = E_{r2}, \quad I_r(t_2) = I_{r2}.
\end{aligned}$$

Table 1 provides explanations of the variables used in the model, whereas Table 2 includes the parameters and their corresponding values.

Table 1: Variables in the system.

The variable	Description
N_h	The population of humans $(S_h + E_h + I_h + Q_h + R_h)$.
S_h	Susceptible class.
E_h	Exposed class.
I_h	Infected class.
Q_h	Isolation class.
R_h	Recovery class.
N_r	The population of rodent $(S_r + E_r + I_r)$.
S_r	Susceptible class.
E_r	Exposed class.
I_r	Infected class.

Table 2: The values of the model's parameters.

Parameter	Description	Value
Λ_h	The recruitment rate of humans	0.34857
Λ_r	The recruitment rate of rodents	0.60822
β_1	The contact rate between rodents and humans	0.00103563
β_2	The contact rate between humans	0.99993476
β_3	The contact rate between rodents	0.50838481
α_1	The transmission rate of humans from exposed to infectious class	0.07296767
α_2	The rate of identification of suspected case	0.00000213
α_3	The transmission rate of rodents from exposed to infectious class	0.03353088
ϕ	The proportion of humans not detected after diagnosis	0.33749119
τ	The rate of transmission from isolation to recovered class	0.99128100
ρ	The recovery rate	0.16786558
μ_h	The natural death rates of humans	$1/(79 \times 365)$
μ_r	The natural death rates of rodents	$1/(5 \times 365)$
δ_h	The disease induced death rates of humans	0.18291202
δ_r	The disease induced death rates of rodents	0.00000255

3.2. The Crossover of Monkeypox Mathematical Model with Exponential Decay Kernel (CM2)

The Caputo-Fabrizio (CF) fractional derivative is an alternative fractional operator introduced to overcome certain limitations of classical fractional derivatives, particularly in handling memory effects with a nonsingular kernel. Applying the Caputo–Fabrizio definition (nonsingular kernel) gives rise to The concept of a system of piecewise differential equations. The Caputo–Fabrizio variable order operator 'κ' is used to extend the deter-

ministic model in $0 < t \leq t_1$, the fractal-fractional of the Caputo–Fabrizio is employed in $t_1 < t \leq t_2$, and the stochastic differential equation (SDE) in $t_2 < t \leq T_f$. Here is an expression for the new model:

$$\begin{aligned}
{}_0^{CF}D_t^{\kappa} S_h &= \Lambda_h^{\kappa} - \frac{(\beta_1^{\kappa} I_r + \beta_2^{\kappa} I_h) S_h}{N_h} - \mu_h^{\kappa} S_h + \phi^{\kappa} Q_h, \\
{}_0^{CF}D_t^{\kappa} E_h &= \frac{(\beta_1^{\kappa} I_r + \beta_2^{\kappa} I_h) S_h}{N_h} - (\gamma_1^{\kappa} + \gamma_2^{\kappa} + \mu_h^{\kappa}) E_h, \\
{}_0^{CF}D_t^{\kappa} I_h &= \gamma_1^{\kappa} E_h - (\mu_h^{\kappa} + \delta_h^{\kappa} + \rho^{\kappa}) I_h, \\
{}_0^{CF}D_t^{\kappa} Q_h &= \gamma_2^{\kappa} E_h - (\phi^{\kappa} + \tau^{\kappa} + \mu_h^{\kappa} + \delta_h^{\kappa}) Q_h, \\
{}_0^{CF}D_t^{\kappa} R_h &= \rho^{\kappa} I_h + \tau^{\kappa} Q_h - \mu_h^{\kappa} R_h, \\
{}_0^{CF}D_t^{\kappa} S_r &= \Lambda_r^{\kappa} - \frac{\beta_3^{\kappa} S_r I_r}{N_r} - \mu_r^{\kappa} S_r, \\
{}_0^{CF}D_t^{\kappa} E_r &= \frac{\beta_3^{\kappa} S_r I_r}{N_r} - (\mu_r^{\kappa} + \gamma_3^{\kappa}) E_r, \\
{}_0^{CF}D_t^{\kappa} I_r &= \gamma_3^{\kappa} E_r - (\mu_r^{\kappa} + \delta_r^{\kappa}) I_r,
\end{aligned} \tag{15}$$

with initial conditions S_{h0}, E_{h0}, I_{h0}, Q_{h0}, R_{h0}, S_{r0}, E_{r0}, I_{r0} at $t = 0$. Furthermore, if $t_1 < t \leq t_2$, the model has the following expression:

$$\begin{aligned}
{}_0^{FFCF}D_t^{\alpha,\beta} S_h &= \Lambda_h^{\alpha} - \frac{(\beta_1^{\alpha} I_r + \beta_2^{\alpha} I_h) S_h}{N_h} - \mu_h^{\alpha} S_h + \phi^{\alpha} Q_h, \\
{}_0^{FFCF}D_t^{\alpha,\beta} E_h &= \frac{(\beta_1^{\alpha} I_r + \beta_2^{\alpha} I_h) S_h}{N_h} - (\gamma_1^{\alpha} + \gamma_2^{\alpha} + \mu_h^{\alpha}) E_h, \\
{}_0^{FFCF}D_t^{\alpha,\beta} I_h &= \gamma_1^{\alpha} E_h - (\mu_h^{\alpha} + \delta_h^{\alpha} + \rho^{\alpha}) I_h, \\
{}_0^{FFCF}D_t^{\alpha,\beta} Q_h &= \gamma_2^{\alpha} E_h - (\phi^{\alpha} + \tau^{\alpha} + \mu_h^{\alpha} + \delta_h^{\alpha}) Q_h, \\
{}_0^{FFCF}D_t^{\alpha,\beta} R_h &= \rho^{\alpha} I_h + \tau^{\alpha} Q_h - \mu_h^{\alpha} R_h, \\
{}_0^{FFCF}D_t^{\alpha,\beta} S_r &= \Lambda_r^{\alpha} - \frac{\beta_3^{\alpha} S_r I_r}{N_r} - \mu_r^{\alpha} S_r, \\
{}_0^{FFCF}D_t^{\alpha,\beta} E_r &= \frac{\beta_3^{\alpha} S_r I_r}{N_r} - (\mu_r^{\alpha} + \gamma_3^{\alpha}) E_r, \\
{}_0^{FFCF}D_t^{\alpha,\beta} I_r &= \gamma_3^{\alpha} E_r - (\mu_r^{\alpha} + \delta_r^{\alpha}) I_r,
\end{aligned} \tag{16}$$

with initial conditions

$$\begin{aligned}
&S_h(t_1) = S_{h1}, \quad E_h(t_1) = E_{h1}, \quad I_h(t_1) = I_{h1}, \quad S_r(t_1) = S_{r1}, \\
&R_h(t_1) = R_{h1}, \quad E_r(r_1) = E_{r1}, \quad Q_h(t_1) = Q_{h1}, \quad I_r(t_1) = I_{r1}.
\end{aligned}$$

Additionally, if $t_2 < t \leq T_f$, the model has the following expression:

$$dS_h = (\Lambda_h - \frac{(\beta_1 I_r + \beta_2 I_h) S_h}{N_h} - \mu_h S_h + \phi Q_h) dt + \sigma_1 S_h dB_1,$$

$$
\begin{aligned}
dE_h &= (\frac{(\beta_1 I_r + \beta_2 I_h)S_h}{N_h} - (\gamma_1 + \gamma_2 + \mu_h)E_h)dt + \sigma_2 E_h dB_2,\\
dI_h &= (\gamma_1 E_h - (\mu_h + \delta_h + \rho)I_h)dt + \sigma_3 I_h dB_3,\\
dQ_h &= (\gamma_2 E_h - (\phi + \tau + \mu_h + \delta_h)Q_h)dt + \sigma_4 Q_h dB_4,\\
dR_h &= (\rho I_h + \tau Q_h - \mu_h R_h)dt + \sigma_5 R_h dB_5,\\
dS_r &= (\Lambda_r - \frac{\beta_3 S_r I_r}{N_r} - \mu_r S_r)dt + \sigma_6 S_r dB_6,\\
dE_r &= (\frac{\beta_3 S_r I_r}{N_r} - (\mu_r + \gamma_3)E_r)dt + \sigma_7 E_r dB_7,\\
dI_r &= (\gamma_3 E_r - (\mu_r + \delta_r)I_r)dt + \sigma_8 I_r dB_8.
\end{aligned} \tag{17}
$$

$$
\begin{aligned}
&S_h(t_2) = S_{h2}, \quad E_h(t_2) = E_{h2}, \quad I_h(t_2) = I_{h2}, \quad Q_h(t_2) = Q_{h2},\\
&R_h(t_2) = R_{h2}, \quad S_r(t_2) = S_{r2}, \quad E_r(r_2) = E_{r2}, \quad I_r(t_2) = I_{r2}.
\end{aligned}
$$

3.3. The Crossover of Monkeypox Mathematical Model with Singular Kernel (CM3)

The Caputo definition of a fractional derivative is one of the most commonly used formulations in fractional calculus, particularly in applications involving physical and engineering problems.

By using the Caputo formulation (singular kernel), the concept of a piecewise differential equation system is introduced. In $0 < t \leq t_1$, the model of deterministic behaviour is extended using the Caputo variable order operator, and in $t_1 < t \leq t_2$, fractal-fractional of caputo variable order is used where the range of $t_2 < t \leq t_f$ contains an expansion of a stochastic differential equation (SDE). The following is an expression for the new model:

$$
\begin{aligned}
{}_0^C D_t^\kappa S_h &= \Lambda_h^\kappa - \frac{(\beta_1^\kappa I_r + \beta_2^\kappa I_h)S_h}{N_h} - \mu_h^\kappa S_h + \phi^\kappa Q_h,\\
{}_0^C D_t^\kappa E_h &= \frac{(\beta_1^\kappa I_r + \beta_2^\kappa I_h)S_h}{N_h} - (\gamma_1^\kappa + \gamma_2^\kappa + \mu_h^\kappa)E_h,\\
{}_0^C D_t^\kappa I_h &= \gamma_1^\kappa E_h - (\mu_h^\kappa + \delta_h^\kappa + \rho^\kappa)I_h,\\
{}_0^C D_t^\kappa Q_h &= \gamma_2^\kappa E_h - (\phi^\kappa + \tau^\kappa + \mu_h^\kappa + \delta_h^\kappa)Q_h,\\
{}_0^C D_t^\kappa R_h &= \rho^\kappa I_h + \tau^\kappa Q_h - \mu_h^\kappa R_h,\\
{}_0^C D_t^\kappa S_r &= \Lambda_r^\kappa - \frac{\beta_3^\kappa S_r I_r}{N_r} - \mu_r^\kappa S_r,\\
{}_0^C D_t^\kappa E_r &= \frac{\beta_3^\kappa S_r I_r}{N_r} - (\mu_r^\kappa + \gamma_3^\kappa)E_r,\\
{}_0^C D_t^\kappa I_r &= \gamma_3^\kappa E_r - (\mu_r^\kappa + \delta_r^\kappa)I_r,
\end{aligned} \tag{18}
$$

with initial conditions $S_{h0}, \quad E_{h0}, \quad I_{h0}, \quad Q_{h0}, \quad R_{h0}, \quad S_{r0}, \quad E_{r0}, \quad I_{r0}$ at $t = 0$.

Furthermore, if $t_1 < t \leq t_2$, the model has the following expression:

$$
\begin{aligned}
{}_0^{FFC}D_t^{\alpha,\beta}S_h &= \Lambda_h^\alpha - \frac{(\beta_1^\alpha I_r + \beta_2^\alpha I_h)S_h}{N_h} - \mu_h^\alpha S_h + \phi^\alpha Q_h,\\
{}_0^{FFC}D_t^{\alpha,\beta}E_h &= \frac{(\beta_1^\alpha I_r + \beta_2^\alpha I_h)S_h}{N_h} - (\gamma_1^\alpha + \gamma_2^\alpha + \mu_h^\alpha)E_h,\\
{}_0^{FFC}D_t^{\alpha,\beta}I_h &= \gamma_1^\alpha E_h - (\mu_h^\alpha + \delta_h^\alpha + \rho^\alpha)I_h,\\
{}_0^{FFC}D_t^{\alpha,\beta}Q_h &= \gamma_2^\alpha E_h - (\phi^\alpha + \tau^\alpha + \mu_h^\alpha + \delta_h^\alpha)Q_h,\\
{}_0^{FFC}D_t^{\alpha,\beta}R_h &= \rho^\alpha I_h + \tau^\alpha Q_h - \mu_h^\alpha R_h,\\
{}_0^{FFC}D_t^{\alpha,\beta}S_r &= \Lambda_r^\alpha - \frac{\beta_3^\alpha S_r I_r}{N_r} - \mu_r^\alpha S_r,\\
{}_0^{FFC}D_t^{\alpha,\beta}E_r &= \frac{\beta_3^\alpha S_r I_r}{N_r} - (\mu_r^\alpha + \gamma_3^\alpha)E_r,\\
{}_0^{FFC}D_t^{\alpha,\beta}I_r &= \gamma_3^\alpha E_r - (\mu_r^\alpha + \delta_r^\alpha)I_r,
\end{aligned}
\tag{19}
$$

with initial conditions

$$
\begin{aligned}
&S_h(t_1) = S_{h1}, \quad E_h(t_1) = E_{h1}, \quad I_h(t_1) = I_{h1}, \quad S_r(t_1) = S_{r1},\\
&R_h(t_1) = R_{h1}, \quad E_r(r_1) = E_{r1}, \quad Q_h(t_1) = Q_{h1}, \quad I_r(t_1) = I_{r1}.
\end{aligned}
$$

Additionally, if $t_2 < t \leq T_f$, the model has the following expression:

$$
\begin{aligned}
dS_h &= (\Lambda_h - \frac{(\beta_1 I_r + \beta_2 I_h)S_h}{N_h} - \mu_h S_h + \phi Q_h)dt + \sigma_1 S_h dB_1,\\
dE_h &= (\frac{(\beta_1 I_r + \beta_2 I_h)S_h}{N_h} - (\gamma_1 + \gamma_2 + \mu_h)E_h)dt + \sigma_2 E_h dB_2,\\
dI_h &= (\gamma_1 E_h - (\mu_h + \delta_h + \rho)I_h)dt + \sigma_3 I_h dB_3,\\
dQ_h &= (\gamma_2 E_h - (\phi + \tau + \mu_h + \delta_h)Q_h)dt + \sigma_4 Q_h dB_4,\\
dR_h &= (\rho I_h + \tau Q_h - \mu_h R_h)dt + \sigma_5 R_h dB_5,\\
dS_r &= (\Lambda_r - \frac{\beta_3 S_r I_r}{N_r} - \mu_r S_r)dt + \sigma_6 S_r dB_6,\\
dE_r &= (\frac{\beta_3 S_r I_r}{N_r} - (\mu_r + \gamma_3)E_r)dt + \sigma_7 E_r dB_7,\\
dI_r &= (\gamma_3 E_r - (\mu_r + \delta_r)I_r)dt + \sigma_8 I_r dB_8.
\end{aligned}
\tag{20}
$$

$$
\begin{aligned}
&S_h(t_2) = S_{h2}, \quad E_h(t_2) = E_{h2}, \quad I_h(t_2) = I_{h2}, \quad S_r(t_2) = S_{r2},\\
&R_h(t_2) = R_{h2}, \quad E_r(r_2) = E_{r2}, \quad Q_h(t_2) = Q_{h2}, \quad I_r(t_2) = I_{r2}.
\end{aligned}
$$

4. Theoretical Analysis of Model

To obtain the equilibrium points of the crossover models, we put all derivatives equal to zero then we have two points as follows:

Disease-free equilibrium [26], when there is no sickness, and given as follows:

$$\epsilon_0 = (\frac{\Lambda_h}{\mu_h}, 0, 0, 0, 0, \frac{\Lambda_r}{\mu_r}, 0, 0). \tag{21}$$

Endemic equilibrium [26] when the virus continues to spread across the population, and given as follows:

$$\epsilon_1 = (S_h^{**}, E_h^{**}, I_h^{**}, Q_h^{**}, R_h^{**}, S_r^{**}, E_r^{**}, I_r^{**})$$

$$\begin{aligned}
S_h^{**} &= \frac{k_1 k_3 \Lambda_h}{\mu_h k_1 k_3 - \alpha_2 \Phi \Phi_h + k_1 k_3 \Phi_h}, \\
E_h^{**} &= \frac{k_3 \Lambda_h \Phi_h}{\mu_h k_1 k_3 - \alpha_2 \Phi \Phi_h + k_1 k_3 \Phi_h}, \\
I_h^{**} &= \frac{k_3 \alpha 1 \Lambda_h \Phi_h}{k_2(\mu_h k_1 k_3 - \alpha_2 \Phi \Phi_h + k_1 k_3 \Phi_h)}, \\
Q_h^{**} &= \frac{\alpha 2 \Lambda_h \Phi_h}{\mu_h k_1 k_3 - \alpha_2 \Phi \Phi_h + k_1 k_3 \Phi_h}, \\
R_h^{**} &= \frac{(k_3 \rho \alpha 1 + k_2 \tau \alpha 2) \Lambda_h \Phi_h}{\mu_h k_2(\mu_h k_1 k_3 - \alpha_2 \Phi \Phi_h + k_1 k_3 \Phi_h)}, \\
S_r^{**} &= \frac{\lambda_r}{\mu_r + \Phi_r}, \\
E_r^{**} &= \frac{\lambda_r}{k_4(\mu_r + \Phi_r)}, \\
I_r^{**} &= \frac{\Phi_r \alpha_3 \lambda_r}{k_4 k_5 (\mu_r + \Phi_r)}.
\end{aligned} \tag{22}$$

The formulas $k_1 = \mu_h + \alpha_2 + \alpha_1$, $k_2 = \rho + \delta_h + \mu_h$, $k_3 = \delta_h + \tau + \mu_h + \Phi$, $k_4 = \alpha_3 + \mu_r$, $k_5 = \delta_r + \mu_r$, $\Phi_h = \frac{\beta_1 I_r^* + \beta_2 T_h^{**}}{N_h}$, $\Phi_r = \frac{\beta_3 I_r^{**}}{N_r}$.

Reproduction number [26]

$$\mathfrak{R}_\circ = \frac{\alpha_1 \beta_2}{(\alpha_1 + \alpha_2 + \mu_h)(\mu_h + \delta_h + \rho)}. \tag{23}$$

Stability of endemic equilibrium point

The Jacobian matrix about the endemic equilibria ϵ_1 is given as:

$$J(\epsilon_1) = \begin{bmatrix}
-(\frac{\beta_1 I_r + \beta_2 I_h}{N_h}) - \mu_h & 0 & -\frac{\beta_2 S_h}{N_h} & \phi & 0 & 0 & 0 & -\frac{\beta_1 S_h}{N_h} \\
\frac{\beta_1 I_r + \beta_2 I_h}{N_h} & -\alpha_1 - \alpha_2 - \mu_h & \frac{\beta_2 S_h}{N_h} & 0 & 0 & 0 & 0 & \frac{\beta_1 S_h}{N_h} \\
0 & \alpha_1 & -\mu_h - \delta_h - \gamma & 0 & 0 & 0 & 0 & 0 \\
0 & \alpha_2 & 0 & -\phi - \tau - \delta_h - \mu_h & 0 & 0 & 0 & 0 \\
0 & 0 & \gamma & \tau & -\mu_h & 0 & 0 & 0 \\
0 & 0 & 0 & 0 & 0 & -\frac{\beta_3 I_r}{N_r} - \mu_r & 0 & -\frac{\beta_3 S_r}{N_r} \\
0 & 0 & 0 & 0 & 0 & \frac{\beta_3 I_r}{N_r} & -\mu_r - \alpha_3 & \frac{\beta_3 S_r}{N_r} \\
0 & 0 & 0 & 0 & 0 & 0 & \alpha_3 & \mu_r - \delta_r
\end{bmatrix},$$

then the characteristic equation of Jacobian is given as:

$$\frac{1}{N_h N_r}\left[(-x-\mu_h)\left(-\phi\alpha_2\left(I_r\beta_1+I_h\beta_2\right)(x+\rho+\delta_h+\mu_h)+(-x-\tau-\phi-\delta_h-\mu_h)\left(S_h\alpha_1\beta_2\left(x+\mu_h\right)\right.\right.\right.$$
$$-(x+\alpha_1+\alpha_2+\mu_h)(x+\rho+\delta_h+\mu_h)(I_r\beta_1+I_h\beta_2+N_h(x+\mu_h))))(S_r\alpha_3\beta_3(x+\mu_r)$$
$$\left.\left.\left.-(x+\alpha_3+\mu_r)\left(I_r\beta_3+N_r(x+\mu_r)\right)(x+(\mu_r+\delta_r))\right)\right)\right]=0. \tag{24}$$

This, when the polynomial is converted to standard form, may be further expressed as follows:

$$x^8+C_1x^7++C_2x^6+C_3x^5+C_4x^4+C_5x^3+C_6x^2+C_7x+C_8=0,$$

where $C_i's$ are the coefficients of $x^{8-i}; i=1,2,\ldots 8$. Therefore, the Monkeypox endemic equilibrium (MFE) is asymptotically stable if $\mathfrak{R}_\circ>1$ and $C_1>0$, $C_1C_2>C_3$, $C_1C_2C_3+C_0C_1C_5>C_0C_3^2+C_1^2C_4$, $P^*Q>PQ^*$, $MQ^*>P^*N$, $M^*N>MN^*$, $XN^*>TM^*$ such that:

$$P=\frac{C_1C_2-C_0C_3}{C_1}, \qquad Q=\frac{C_1C_4-C_0C_5}{C_1}$$
$$R=\frac{C_1C_6-C_0C_7}{C_1}, \qquad S=C_8$$
$$P^*=\frac{PC_3-C_1Q}{P}, \qquad Q^*=\frac{PC_5-C_1R}{P}$$
$$R^*=\frac{PC_7-C_1S}{P}, \qquad M=\frac{P^*Q-PQ^*}{P^*}$$
$$N=\frac{P^*R-PR^*}{P^*}, \qquad T=\frac{PS}{P^*}$$
$$M^*=\frac{MQ^*-P^*N}{M}, \qquad N^*=\frac{MR^*-P^*T}{M}$$
$$X=\frac{M^*N-MN^*}{M^*}.$$

5. Numerical Schemes for Crossover Models

5.1. Numerical Scheme with Nonsingular Kernel

In this section, we will present the numerical methods to solve the crossover models with nonsingular kernel (12)-(14) and (15)-(17) and the crossover model with singular kernel (18)-(20) as follows:

5.1.1. Toufik-Atangana method

Consider the general formula of the variable-order Atangana-Baleanu differential equation given in $(0,t_1]$ as follows:

$${}_0^{ABC}D_t^{\kappa}Y(t)=f(t,Y(t)), \quad Y(0)=Y_0, \quad \kappa=\alpha(t)\in(0,1]. \tag{25}$$

By integrate (25) using (5). Then by using the approximation of the variable-order Atangana-Baleanu integral equation and Lagrange polynomial of two step we have the following formula to approximate the variable-order Atangana-Baleanu differential equation [21]:

$$\begin{aligned}
Y_{p+1} = Y_0 + \frac{1-\kappa}{AB(\kappa)} f(t_p, Y_p) + \frac{\kappa h^\kappa}{AB(\kappa)\Gamma(\kappa+2)} \sum_{s=0}^{p} f(t_p, Y_p)[(-s+1+p)^\kappa \\
(-s+p+\kappa+2) - (-s+p)^\kappa(-s+p+2\kappa+2)] - \frac{\kappa h^\kappa}{AB(k)\Gamma(\kappa+2)} \\
\sum_{s=0}^{p}[(-s+p+1)^{\kappa+1} - (-s+p)^\kappa(-s+p+\kappa+1)] f(t_{s-1}, Y_{s-1}). \qquad (26)
\end{aligned}$$

When the suggested numerical method (26) is applied to system (12), the outcomes are

$$\begin{aligned}
S_{hp+1} &= S_{h0} + \frac{1-\kappa}{AB(\kappa)}(\Lambda_h - \frac{(\beta_1 I_{rp} + \beta_2 I_{hp})S_{hp}}{N_{hp}} - \mu_h S_{hp} + \phi Q_{hp}) + \frac{\kappa h^\kappa}{AB(\kappa)\Gamma(\kappa+2)} \\
&\times \sum_{s=0}^{p}(\Lambda_h - \frac{(\beta_1 I_{rs} + \beta_2 I_{hs})S_{hs}}{N_{hs}} - \mu_h S_{hs} + \phi Q_{hs})[(-s+p+1)^\kappa(-s+\kappa+2+p) \\
&- (-s+p)^\kappa(-s+2\kappa+2+p)] - \frac{\kappa h^\kappa}{AB(\kappa)\Gamma(\kappa+2)} \sum_{s=0}^{p} \Big[\Lambda_h - \frac{(\beta_1 I_{r(s-1)} + \beta_2 I_{h(s-1)})}{N_{h(s-1)}} \\
&S_{h(s-1)} - \mu_h S_{h(s-1)} + \phi Q_{h(s-1)}\Big] [(-s+p+1)^{\kappa+1} - (-s+p)^\kappa(-s+\kappa+1+p)], \\
E_{hp+1} &= E_{h0} + \frac{1-\kappa}{AB(\kappa)}(\frac{(\beta_1 I_{rp} + \beta_2 I_{hp})S_{hp}}{N_{hp}} - (\gamma_1+\gamma_2+\mu_h)E_{hp}) + \frac{\kappa h^\kappa}{AB(\kappa)\Gamma(\kappa+2)} \\
&\times \sum_{s=0}^{p}(\frac{(\beta_1 I_{rs} + \beta_2 I_{hs})S_{hs}}{N_{hs}} - (\gamma_1+\gamma_2+\mu_h)E_{hs})[(-s+p+1)^\kappa(-s+p+2+\kappa) \\
&- (-s+p)^\kappa(-s+2+2\kappa+p)] - \frac{\kappa h^\kappa}{AB(\kappa)\Gamma(\kappa+2)} \sum_{s=0}^{p} \Big[\frac{(\beta_1 I_{r(s-1)} + \beta_2 I_{h(s-1)})}{N_{h(s-1)}} \\
&*S_{h(s-1)} - (\gamma_1+\gamma_2+\mu_h)E_{h(s-1)}\Big] [(-s+p+1)^{\kappa+1} - (-s+p)^\kappa(-s+\kappa+1+p)], \\
I_{hp+1} &= I_{h0} + \frac{1-\kappa}{AB(\kappa)}(\gamma_1 E_{hp} - (\mu_h+\delta_h+\rho)I_{hp}) + \frac{\kappa h^\kappa}{AB(\kappa)\Gamma(\kappa+2)} \sum_{s=0}^{p} [\gamma_1 E_{hs} \\
&-(\mu_h+\delta_h+\rho)I_{hs}] [(-s+p+1)^\kappa(-s+\kappa+2+p) - (-s+p)^\kappa(-s+2\kappa+2+p)] \\
&- \frac{\kappa h^\kappa}{AB(\kappa)\Gamma(\kappa+2)} \sum_{s=0}^{p}(\gamma_1 E_{h(s-1)} - (\mu_h+\delta_h+\rho)I_{h(s-1)}) \left[(-s+p+1)^{\kappa+1}\right. \\
&\left.-(-s+p)^\kappa(-s+1+\kappa+p)\right], \\
Q_{hp+1} &= Q_{h0} + \frac{1-\kappa}{AB(\kappa)}(\gamma_2 E_{hp} - (\phi+\tau+\mu_h+\delta_h)Q_{hp}) + \frac{\kappa h^\kappa}{AB(\kappa)\Gamma(\kappa+2)} \sum_{s=0}^{p} [\gamma_2 E_{hs}
\end{aligned}$$

$$
\begin{aligned}
&-(\phi+\tau+\mu_h+\delta_h)Q_{hs}]\,[(-s+p+1)^{\kappa}(-s+p+\kappa+2)-(-s+p)^{\kappa}(-s+p+2\kappa+2)]\\
&-\frac{\kappa h^{\kappa}}{AB(\kappa)\Gamma(\kappa+2)}\sum_{s=0}^{p}(\gamma_2 E_{h(s-1)}-(\phi+\tau+\mu_h+\delta_h)Q_{h(s-1)})[(-s+p+1)^{\kappa+1}\\
&-(-s+p)^{\kappa}(-s+p+1+\kappa)],\\
R_{hp+1}&=R_{h0}+\frac{1-\kappa}{AB(\kappa)}(\rho I_{hp}+\tau Q_{hp}-\mu_h R_{hp})+\frac{\kappa h^{\kappa}}{AB(\kappa)\Gamma(\kappa+2)}\sum_{s=0}^{p}(\rho I_{hs}+\tau Q_{hs}-\mu_h R_{hs})\\
&[(-s+p+1)^{\kappa}(-s+2+\kappa+p)-(-s+p)^{\kappa}(-s+2+2\kappa+p)]-\frac{\kappa h^{\kappa}}{AB(\kappa)\Gamma(\kappa+2)}\\
&\times\sum_{s=0}^{p}(\rho I_{h(s-1)}+\tau Q_{h(s-1)}-\mu_h R_{h(s-1)})[(-s+1+p)^{\kappa+1}-(-s+p)^{\kappa}(-s+\kappa+1+p)],\\
S_{rp+1}&=S_{r0}+\frac{1-\kappa}{AB(\kappa)}(\Lambda_r-\frac{\beta_3 S_{rp}I_{rp}}{N_{rp}}-\mu_r S_{rp})+\frac{h^{\kappa}\kappa}{\Gamma(2+\kappa)AB(\kappa)}\sum_{s=0}^{p}\Big[\Lambda_h-\frac{\beta_3 S_{rs}I_{rs}}{N_{rs}}\\
&-\mu_r S_{rs}]\,[(-s+p+1)^{\kappa}(-s+\kappa+2+p)-(-s+p)^{\kappa}(-s+2\kappa+2+p)]\\
&-\frac{\kappa h^{\kappa}}{AB(\kappa)\Gamma(\kappa+2)}\sum_{s=0}^{p}(\Lambda_h-\frac{\beta_3 S_{r(s-1)}I_{r(s-1)}}{N_{r(s-1)}}-\mu_r S_{r(s-1)})[(-s+p+1)^{\kappa+1}\\
&-(-s+p)^{\kappa}(-s+p+\kappa+1)],\\
E_{rp+1}&=E_{r0}+\frac{1-\kappa}{AB(\kappa)}(\frac{\beta_3 S_{rp}I_r}{N_{rp}}-(\mu_r+\gamma_3)E_{rp})+\frac{\kappa h^{\kappa}}{AB(\kappa)\Gamma(\kappa+2)}\sum_{s=0}^{p}\Big[\frac{\beta_3 S_{rs}I_{rs}}{N_{rs}}\\
&-(\mu_r+\gamma_3)E_{rs}]\,[(-s+p+1)^{\kappa}(-s+\kappa+2+p)-(-s+2)^{\kappa}(-s+2\kappa+2+p)]\\
&-\frac{\kappa h^{\kappa}}{AB(\kappa)\Gamma(\kappa+2)}\sum_{s=0}^{p}(\frac{\beta_3 S_{r(s-1)}I_{r(s-1)}}{N_{r(s-1)}}-(\mu_r+\gamma_3)E_{r(s-1)})[(-s+p+1)^{\kappa+1}\\
&-(-s+p)^{\kappa}(-s+p+\kappa+1)],\\
I_{rp+1}&=I_{r0}+\frac{1-\kappa}{AB(\kappa)}(\gamma_3 E_{rp}-(\mu_r+\delta_r)I_{rp})+\frac{\alpha(t)h^{\kappa}}{AB(\kappa)\Gamma(\kappa+2)}\sum_{s=0}^{p}[\gamma_3 E_{rs}-(\mu_r+\delta_r)I_{rs}]\\
&[(-s+p+1)^{\kappa}(-s+p+2+\kappa)-(-s+p)^{\kappa}(-s+p+2\kappa+2)]-\frac{\kappa h^{\kappa}}{AB(\kappa)\Gamma(\kappa+2)}\\
&\times\sum_{s=0}^{p}(\gamma_3 E_{r(s-1)}-(\mu_r+\delta_r)I_{r(s-1)})[(-s+p+1)^{\kappa+1}-(-s+p)^{\kappa}(-s+p+\kappa+1)].
\end{aligned}
\tag{27}
$$

Now consider the general formula for fractal-fractional Atangana-Baleanu deferential equation in the $(t_1, t_2]$ given as follows:

$$
{}_0^{FFABC}D_t^{\alpha,\beta}Y(t)=f(t,Y(t)),\quad Y(0)=Y_0,\quad \alpha,\beta\in(0,1]. \tag{28}
$$

243 Using [21] the approximation of (28) is given as follows:

$$Y_{p+1} = Y_0 + \frac{1-\alpha}{AB(\alpha)} t_p^{\beta-1} f(t_p, Y_p) + \frac{\alpha\beta h^\alpha}{AB(\alpha)\Gamma(\alpha+2)} \sum_{s=0}^{p} t_p^{\beta-1} f(t_p, Y_p) \left[(-s+p+1)^\alpha(-s+p+\alpha+2)\right.$$
$$\left.-(-s+p)^\alpha(-s+p+2\alpha+2)\right] - \frac{\alpha\beta h^\alpha}{AB(\alpha)\Gamma(\alpha+2)} \sum_{s=0}^{p} t_{s-1}^{\beta-1} f(t_{s-1}, Y_{s-1}) \left[(-s+p+1)^{\alpha+1}\right.$$
$$\left.-(-s+\alpha+p+1)(-s+p)^\alpha\right]. \tag{29}$$

244 Utilising the proposed numerical technique TAM (5.1.1) in the system (13), we obtain:

$$S_{hp+1} = S_{h0} + \frac{1-\alpha}{AB(\alpha)} t_p^{\beta-1}(\Lambda_h - \frac{(\beta_1 I_{rp} + \beta_2 I_{hp}) S_{hp}}{N_{hp}} - \mu_h S_{hp} + \phi Q_{hp}) + \frac{\alpha\beta h^\alpha}{AB(\alpha)\Gamma(\alpha+2)}$$
$$\times \sum_{s=0}^{p} t_p^{\beta-1}(\Lambda_h - \frac{(\beta_1 I_{rs} + \beta_2 I_{hs}) S_{hs}}{N_{hs}} - \mu_h S_{hs} + \phi Q_{hs})[(-s+\alpha+2+p)(-s+p+1)^\alpha$$
$$- (-s+p)^\alpha(-s+2\alpha+2+p)] - \frac{\alpha\beta h^\alpha}{AB(\alpha)\Gamma(\alpha+2)} \sum_{s=0}^{p} t_{s-1}^{\beta-1} \left[\Lambda_h - \frac{(\beta_1 I_{r(s-1)} + \beta_2 I_{h(s-1)})}{N_{h(s-1)}}\right.$$
$$\left. S_{h(s-1)} - \mu_h S_{h(s-1)} + \phi Q_{h(s-1)}\right] [(-s+1+p)^{\alpha+1} - (-s+p)^\alpha(-s+\alpha+1+p)],$$
$$E_{hp+1} = E_{h0} + \frac{1-\alpha}{AB(\alpha)} t_p^{\beta-1}(\frac{(\beta_1 I_{rp} + \beta_2 I_{hp}) S_{hp}}{N_{hp}} - (\gamma_1+\gamma_2+\mu_h) E_{hp}) + \frac{\alpha\beta h^\alpha}{AB(\alpha)\Gamma(\alpha+2)}$$
$$\times \sum_{s=0}^{p} t_p^{\beta-1}(\frac{(\beta_1 I_{rs} + \beta_2 I_{hs}) S_{hs}}{N_{hs}} - (\gamma_1+\gamma_2+\mu_h) E_{hs})[(-s+p+1)^\alpha(-s+\alpha+2+p)$$
$$- (-s+p)^\alpha(-s+2\alpha+2+p)] - \frac{\alpha\beta h^\alpha}{AB(\alpha)\Gamma(\alpha+2)} \sum_{s=0}^{p} t_{s-1}^{\beta-1}(\frac{(\beta_1 I_{r(s-1)} + \beta_2 I_{h(s-1)}) S_{h(s-1)}}{N_{h(s-1)}}$$
$$- (\gamma_1+\gamma_2+\mu_h) E_{h(s-1)})[(-s+p+1)^{\alpha+1} - (-s+\alpha+1+p)(-s+p)^\alpha],$$
$$I_{hp+1} = I_{h0} + \frac{1-\alpha}{AB(\alpha)} t_p^{\beta-1}(\gamma_1 E_{hp} - (\mu_h+\delta_h+\rho) I_{hp}) + \frac{\alpha\beta h^\alpha}{AB(\alpha)\Gamma(\alpha+2)} \sum_{s=0}^{p} t_p^{\beta-1} [\gamma_1 E_{hs}$$
$$-(\mu_h+\delta_h+\rho) I_{hs}] [(-s+p+1)^\alpha(-s+p+\alpha+2) - (-s+p)^\alpha(-s+p+2\alpha+2)]$$
$$- \frac{\alpha\beta h^\alpha}{AB(\alpha)\Gamma(\alpha+2)} \sum_{s=0}^{p} t_{s-1}^{\beta-1}(\gamma_1 E_{h(s-1)} - (\mu_h+\delta_h+\rho) I_{h(s-1)})[(-s+p+1)^{\alpha+1}$$
$$- (-s+p)^\alpha(-s+p+1+\alpha)],$$
$$Q_{hp+1} = Q_{h0} + \frac{1-\alpha}{AB(\alpha)} t_p^{\beta-1}(\gamma_2 E_{hp} - (\phi+\tau+\mu_h+\delta_h) Q_{hp}) + \frac{\alpha\beta h^\alpha}{AB(\alpha)\Gamma(\alpha+2)} \sum_{s=0}^{p} t_p^{\beta-1} [\gamma_2 E_{hs}$$
$$-(\phi+\tau+\mu_h+\delta_h) Q_{hs}] [(-s+p+1)^\alpha(-s+2+\alpha+p) - (-s+p+2+2\alpha)(-s+p)^\alpha]$$
$$- \frac{\alpha\beta h^\alpha}{AB(\alpha)\Gamma(\alpha+2)} \sum_{s=0}^{p} t_{s-1}^{\beta-1}(\gamma_2 E_{h(s-1)} - (\phi+\tau+\mu_h+\delta_h) Q_{h(s-1)})[(-s+1+p)^{\alpha+1}$$

$$
\begin{aligned}
&- (-s+p)^{\alpha}(-s+\alpha+1+p)],\\
R_{hp+1} &= R_{h0} + \frac{1-\alpha}{AB(\alpha)} t_p^{\beta-1}(\rho I_{hp} + \tau Q_{hp} - \mu_h R_{hp}) + \frac{h^{\alpha}\alpha\beta}{\Gamma(\alpha+2)AB(\alpha)} \sum_{s=0}^{p} t_p^{\beta-1} [\rho I_{hs} + \tau Q_{hs}\\
&-\mu_h R_{hs}] [(-s+2+\alpha+p)(-s+1+p)^{\alpha} - (-s+2+2\alpha+p)(-s+p)^{\alpha}] - \frac{\alpha\beta h^{\alpha}}{AB(\alpha)\Gamma(\alpha+2)}\\
&\times \sum_{s=0}^{p} t_{s-1}^{\beta-1}(\rho I_{h(s-1)} + \tau Q_{h(s-1)} - \mu_h R_{h(s-1)})[-(-s+p+1+\alpha)(-s+p)^{\alpha} + (-s+p+1)^{\alpha+1}],\\
S_{rp+1} &= S_{r0} + \frac{1-\alpha}{AB(\alpha)} t_p^{\beta-1}(\Lambda_r - \frac{\beta_3 S_{rp} I_{rp}}{N_{rp}} - \mu_r S_{rp}) + \frac{\alpha\beta h^{\alpha}}{AB(\alpha)\Gamma(\alpha+2)} \sum_{s=0}^{p} t_p^{\beta-1}(\Lambda_h - \frac{\beta_3 S_{rs} I_{rs}}{N_{rs}}\\
&- \mu_r S_{rs})[(-s+p+2+\alpha)(-s+p+1)^{\alpha} - (-s+2+2\alpha+p)(-s+p)^{\alpha}] - \frac{\alpha\beta h^{\alpha}}{AB(\alpha)\Gamma(\alpha+2)}\\
&\times \sum_{s=0}^{p} t_{s-1}^{\beta-1}(\Lambda_h - \frac{\beta_3 S_{r(s-1)} I_{r(s-1)}}{N_{r(s-1)}} - \mu_r S_{r(s-1)})[(-s+1+p)^{\alpha+1} - (-s+p)^{\alpha}(-s+1+\alpha+p)],\\
E_{rp+1} &= E_{r0} + \frac{1-\alpha}{AB(\alpha)} t_p^{\beta-1}(\frac{\beta_3 S_{rp} I_r}{N_{rp}} - (\mu_r+\gamma_3)E_{rp}) + \frac{\alpha\beta h^{\alpha}}{AB(\alpha)\Gamma(\alpha+2)} \sum_{s=0}^{p} t_p^{\beta-1}(\frac{\beta_3 S_{rs} I_{rs}}{N_{rs}}\\
&- (\mu_r+\gamma_3)E_{rs})[(-s+1+p)^{\alpha}(-s+2+\alpha+p) - (-s+p)^{\alpha}(-s+2+2\alpha+p)] - \frac{\alpha\beta h^{\alpha}}{AB(\alpha)\Gamma(\alpha+2)}\\
&\times \sum_{s=0}^{p} t_{s-1}^{\beta-1}(\frac{\beta_3 S_{r(s-1)} I_{r(s-1)}}{N_{r(s-1)}} - (\mu_r+\gamma_3)E_{r(s-1)})[(-s+1+p)^{\alpha+1} - (-s+p)^{\alpha}(-s+1+\alpha+p)],\\
I_{rp+1} &= I_{r0} + \frac{1-\alpha}{AB(\alpha)} t_p^{\beta-1}(\gamma_3 E_{rp} - (\mu_r+\delta_r)I_{rp}) + \frac{\alpha\beta h^{\alpha}}{AB(\alpha)\Gamma(\alpha+2)} \sum_{s=0}^{p} t_p^{\beta-1}(\gamma_3 E_{rs} - (\mu_r+\delta_r)I_{rs})\\
&[(-s+p+1)^{\alpha}(-s+2+\alpha+p) - (-s+2+2\alpha+p)(-s+p)^{\alpha}] - \frac{\alpha\beta h^{\alpha}}{AB(\alpha)\Gamma(\alpha+2)}\\
&\times \sum_{s=0}^{p} t_{s-1}^{\beta-1}(\gamma_3 E_{r(s-1)} - (\mu_r+\delta_r)I_{r(s-1)})[(-s+1+p)^{\alpha+1} - (-s+p)^{\alpha}(-s+1+\alpha+p)].
\end{aligned}
\tag{30}
$$

Remark 5.1. *The stability and error analysis for this method are found in [21].*

During the third interval $(t_2, T_f])$, to approximate the system (14), we will use Milstein method (11). Then the explicit solution given as follows:

$$
\begin{aligned}
S_{hp+1} &= S_{hp} + (\Lambda_h - \frac{(\beta_1 I_r + \beta_2 I_h)S_h}{N_h} - \mu_h S_h + \phi Q_h)h + \sigma_1 S_{hp}\Delta B_p + 0.5\sigma_1^2 S_{hp}\\
&((\Delta B_p)^2 - h),
\end{aligned}
$$

$$
\begin{aligned}
E_{hp+1} &= E_{hp} + (\frac{(\beta_1 I_r + \beta_2 I_h)S_h}{N_h} - (\gamma_1 + \gamma_2 + \mu_h)E_h)h + \sigma_2 E_{hp}\Delta B_p + 0.5\sigma_2^2 E_{hp} \\
&\quad ((\Delta B_p)^2 - h), \\
I_{hp+1} &= I_{hp} + (\gamma_1 E_h - (\mu_h + \delta_h + \rho)I_h)h + \sigma_3 I_{hp}\Delta B_p + 0.5\sigma_3^2 I_{hp}((\Delta B_p)^2 - h), \\
Q_{hp+1} &= Q_{hp} + (\gamma_2 E_h - (\phi + \tau + \mu_h + \delta_h)Q_h)h + \sigma_4 Q_{hp}\Delta B_p + 0.5\sigma_4^2 Q_{hp}((\Delta B_p)^2 - \phi h), \\
R_{hp+1} &= R_{hp} + (\rho I_h + \tau Q_h - \mu_h R_h)\phi h + \sigma_5 * R_{hp}\Delta B_p + 0.5\sigma_5^2 R_{hp}((\Delta B_p)^2 - h), \\
S_{rp+1} &= S_{rp} + (\Lambda_r - \frac{\beta_3 S_r I_r}{N_r} - \mu_r S_r)h + \sigma_6 S_{rp}\Delta B_p + 0.5\sigma_6^2 S_{rp}((\Delta B_p)^2 - h), \\
E_{rp+1} &= E_{rp} + (\frac{\beta_3 S_r I_r}{N_r} - (\mu_r + \gamma_3)E_r)h + \sigma_7 E_{rp}\Delta B_p + 0.5\sigma_7^2 E_{rp}((\Delta B_p)^2 - h), \\
I_{rp+1} &= I_{rp} + (\gamma_3 E_r - (\mu_r + \delta_r)I_r)h + \sigma_8 I_{rp}\Delta B_p + 0.5\sigma_8^2 I_{rp}((\Delta B_p)^2 - h).
\end{aligned} \tag{31}
$$

5.2. Numerical Scheme with Exponential Decay Kernel

Consider the general formula of the variable-order Caputo Fabrizo variable-order differential equation in $(0, t_1]$ as follows:

$$
{}_0^{CF}D_t^{\kappa} Y(t) = f(t, Y(t)), \quad Y(0) = Y_0, \quad \kappa = \alpha(t) \in (0, 1]. \tag{32}
$$

First integrate (32) using (9). Then by using the approximation of the variable-order Caputo Fabrizo integral equation and Lagrange polynomial of two step we have the following formula to approximate the variable-order Caputo Fabrizo differential equation [21]:

$$
Y_{p+1} = Y_p + \frac{1-\kappa}{M(\kappa)}[f(t_p, Y_p) - f(t_{p-1}, Y_{p-1})] + \frac{\kappa}{M(\kappa)}[f(t_p, Y_p)\frac{3}{2}h - f(t_{p-1}, Y_{p-1})\frac{1}{2}h]. \tag{33}
$$

Applying the recommended numerical approach (33) to approximate the system (17) yields the following results:

$$
\begin{aligned}
S_{hp+1} &= S_{hp} + (\frac{1-\kappa}{M(\kappa)} + h\frac{3\kappa}{2M(\kappa)})(\Lambda_h - \frac{(\beta_1 I_{rp} + \beta_2 I_{hp})S_{hp}}{N_{hp}} - \mu_h S_{hp} + \phi Q_{hp}) \\
&\quad - (\frac{1-\kappa}{M(\kappa)} + \frac{\kappa}{2M(\kappa)}h)(\Lambda_h - \frac{(\beta_1 I_{r(p-1)} + \beta_2 I_{h(p-1)})S_{h(p-1)}}{N_{h(p-1)}} - \mu_h S_{h(p-1)} + \phi Q_{h(p-1)}), \\
E_{hp+1} &= E_{hp} + (\frac{1-\kappa}{M(\kappa)} + h\frac{3\kappa}{2M(\kappa)})(\frac{(\beta_1 I_{rp} + \beta_2 I_{hp})S_{hp}}{N_{hp}} - (\gamma_1 + \gamma_2 + \mu_h)E_{hp}) \\
&\quad - (\frac{1-\kappa}{M(\kappa)} + \frac{\kappa}{2M(\kappa)}h)(\frac{(\beta_1 I_{r(p-1)} + \beta_2 I_{h(p-1)})S_{h(p-1)}}{N_{h(p-1)}} - (\gamma_1 + \gamma_2 + \mu_h)E_{h(p-1)}), \\
I_{hp+1} &= I_{hp} + (\frac{1-\kappa}{M(\kappa)} + h\frac{3\kappa}{2M(\kappa)})(\gamma_1 E_{hp} - (\mu_h + \delta_h + \rho)I_{hp}) \\
&\quad - (\frac{1-\kappa}{M(\kappa)} + \frac{\kappa}{2M(\kappa)}h)(\gamma_1 E_{hp-1} - (\mu_h + \delta_h + \rho)I_{hp-1}),
\end{aligned}
$$

$$
\begin{aligned}
Q_{hp+1} &= Q_{hp} + (\frac{1-\kappa}{M(\kappa)} + h\frac{3\kappa}{2M(\kappa)})(\gamma_2 E_{hp} - (\phi+\tau+\mu_h+\delta_h)Q_{hp}) \\
&\quad - (\frac{1-\kappa}{M(\kappa)} + \frac{\kappa}{2M(\kappa)}h)(\gamma_2 E_{h(p-1)} - (\phi+\tau+\mu_h+\delta_h)Q_{h(p-1)}), \\
R_{hp+1} &= R_{hp} + (\frac{1-\kappa}{M(\kappa)} + h\frac{3\kappa}{2M(\kappa)})(\rho I_{hp} + \tau Q_{hp} - \mu_h R_{hp}) \\
&\quad - (\frac{1-\kappa}{M(\kappa)} + \frac{\kappa}{2M(\kappa)}h)(\rho I_{h(p-1)} + \tau Q_{h(p-1)} - \mu_h R_{h(p-1)}), \\
S_{rp+1} &= S_{rp} + (\frac{1-\kappa}{M(\kappa)} + h\frac{3\kappa}{2M(\kappa)})(\Lambda_r - \frac{\beta_3 S_{rp} I_{rp}}{N_{rp}} - \mu_r S_{rp}) \\
&\quad - (\frac{-\kappa+1}{M(\kappa)} + h\frac{\kappa}{2M(\kappa)})\frac{\beta_3 S_{r(p-1)} I_{r(p-1)}}{N_{r(p-1)}} - \mu_r S_{r(p-1)}), \\
E_{rp+1} &= E_{rp} + (\frac{1-\kappa}{M(\kappa)} + h\frac{3\kappa}{2M(\kappa)})(\frac{\beta_3 S_{rp} I_r}{N_{rp}} - (\mu_r+\gamma_3)E_{rp}) \\
&\quad - (\frac{1-\kappa}{M(\kappa)} + \frac{\kappa}{2M(\kappa)}h)(\frac{\beta_3 S_{r(p-1)} I_{r(p-1)}}{N_{r(p-1)}} - (\mu_r+\gamma_3)E_{r(p-1)}), \\
I_{rp+1} &= I_{rp} + (\frac{1-\kappa}{M(\kappa)} + h\frac{3\kappa}{2M(\kappa)})(\gamma_3 E_{rp} - (\mu_r+\delta_r)I_{rp}) \\
&\quad - (\frac{1-\kappa}{M(\kappa)} + \frac{\kappa}{2M(\kappa)}h)(\gamma_3 E_{r(p-1)} - (\mu_r+\delta_r)I_{r(p-1)}).
\end{aligned}
\tag{34}
$$

Consider the general formula for fractal-fractional Caputo Fabrizo defferential equation in the $(t_1, t_2]$ given as follows:

$$
{}_0^{FFCF}D_t^{\alpha,\beta} Y(t) = f(t, Y(t)), \quad Y(0) = Y_0, \quad \alpha, \beta \in (0, 1]. \tag{35}
$$

Using [21] the approximation of (35) is given as follows:

$$
\begin{aligned}
Y_{p+1} &= Y_p + \frac{1-\alpha}{M(\alpha)}[\beta t_p^{\beta-1} f(t_p, Y_p) - \beta t_{p-1}^{\beta-1} f(t_{p-1}, Y_{p-1})] + \frac{\alpha}{M(\alpha)}\left[\beta t_p^{\beta-1} f(t_p, Y_p)\frac{3}{2}h\right. \\
&\quad \left. -\beta t_p^{\beta-1} f(t_{p-1}, Y_{p-1})\frac{1}{2}h\right].
\end{aligned}
\tag{36}
$$

Applying the recommended numerical approach (36) to the system (16) yields the following results:

$$
\begin{aligned}
S_{hp+1} &= S_{hp} + (\frac{1-\alpha}{M(\alpha)} + \frac{3\alpha}{2M(\alpha)}h)(\beta t_p^{\beta-1})(\Lambda_h - \frac{(\beta_1 I_{rp} + \beta_2 I_{hp})S_{hp}}{N_{hp}} - \mu_h S_{hp} + \phi Q_{hp}) - (\frac{1-\alpha}{M(\alpha)} \\
&\quad + \frac{\alpha}{2M(\alpha)}h)(\beta t_p^{\beta-1})(\Lambda_h - \frac{(\beta_1 I_{r(p-1)} + \beta_2 I_{h(p-1)})S_{h(p-1)}}{N_{h(p-1)}} - \mu_h S_{h(p-1)} + \phi Q_{h(p-1)}), \\
E_{hp+1} &= E_{hp} + (\frac{1-\alpha}{M(\alpha)} + \frac{3\alpha}{2M(\alpha)}h)(\beta t_p^{\beta-1})(\frac{(\beta_1 I_{rp} + \beta_2 I_{hp})S_{hp}}{N_{hp}} - (\gamma_1+\gamma_2+\mu_h)E_{hp})
\end{aligned}
$$

$$
\begin{aligned}
&- (\frac{1-\alpha}{M(\alpha)} + \frac{\alpha}{2M(\alpha)}h)(\beta t_p^{\beta-1})(\frac{(\beta_1 I_{r(p-1)} + \beta_2 I_{h(p-1)})S_{h(p-1)}}{N_{h(p-1)}} - (\gamma_1 + \gamma_2 + \mu_h)E_{h(p-1)}),\\
I_{hp+1} &= I_{hp} + (\frac{1-\alpha}{M(\alpha)} + \frac{3\alpha}{2M(\alpha)}h)(\beta t_p^{\beta-1})(\gamma_1 E_{hp} - (\mu_h + \delta_h + \rho)I_{hp})\\
&- (\frac{1-\alpha}{M(\alpha)} + \frac{\alpha}{2M(\alpha)}h)(\beta t_p^{\beta-1})(\gamma_1 E_{hp-1} - (\mu_h + \delta_h + \rho)I_{hp-1}),\\
Q_{hp+1} &= Q_{hp} + (\frac{1-\alpha}{M(\alpha)} + \frac{3\alpha}{2M(\alpha)}h)(\beta t_p^{\beta-1})(\gamma_2 E_{hp} - (\phi + \tau + \mu_h + \delta_h)Q_{hp})\\
&- (\frac{1-\alpha}{M(\alpha)} + \frac{\alpha}{2M(\alpha)}h)(\beta t_p^{\beta-1})(\gamma_2 E_{h(p-1)} - (\phi + \tau + \mu_h + \delta_h)Q_{h(p-1)}),\\
R_{hp+1} &= R_{hp} + (\frac{1-\alpha}{M(\alpha)} + \frac{3\alpha}{2M(\alpha)}h)(\beta t_p^{\beta-1})(\rho I_{hp} + \tau Q_{hp} - \mu_h R_{hp})\\
&- (\frac{1-\alpha}{M(\alpha)} + \frac{\alpha}{2M(\alpha)}h)(\beta t_p^{\beta-1})(\rho I_{h(p-1)} + \tau Q_{h(p-1)} - \mu_h R_{h(p-1)}),\\
S_{rp+1} &= S_{rp} + (\frac{1-\alpha}{M(\alpha)} + \frac{3\alpha}{2M(\alpha)}h)(\beta t_p^{\beta-1})(\Lambda_r - \frac{\beta_3 S_{rp} I_{rp}}{N_{rp}} - \mu_r S_{rp})\\
&- (\frac{1-\alpha}{M(\alpha)} + \frac{\alpha}{2M(\alpha)}h)(\beta t_p^{\beta-1})(\frac{\beta_3 S_{r(p-1)} I_{r(p-1)}}{N_{r(p-1)}} - \mu_r S_{r(p-1)}),\\
E_{rp+1} &= E_{rp} + (\frac{1-\alpha}{M(\alpha)} + \frac{3\alpha}{2M(\alpha)}h)(\beta t_p^{\beta-1})(\frac{\beta_3 S_{rp} I_r}{N_{rp}} - (\mu_r + \gamma_3)E_{rp})\\
&- (\frac{1-\alpha}{M(\alpha)} + \frac{\alpha}{2M(\alpha)}h)(\beta t_p^{\beta-1})(\frac{\beta_3 S_{r(p-1)} I_{r(p-1)}}{N_{r(p-1)}} - (\mu_r + \gamma_3)E_{r(p-1)}),\\
I_{rp+1} &= I_{rp} + (\frac{1-\alpha}{M(\alpha)} + \frac{3\alpha}{2M(\alpha)}h)(\beta t_p^{\beta-1})(\gamma_3 E_{rp} - (\mu_r + \delta_r)I_{rp})\\
&- (\frac{1-\alpha}{M(\alpha)} + \frac{\alpha}{2M(\alpha)}h)(\beta t_p^{\beta-1})(\gamma_3 E_{r(p-1)} - (\mu_r + \delta_r)I_{r(p-1)}).
\end{aligned}
\tag{37}
$$

Remark 5.2. *The stability and error analysis for this method are found in [21].*

The third interval $(t_2, T_f]$), to approximate the system (17), we will use Milstein method (11). Then the explicit solution given as follows:

$$
\begin{aligned}
S_{hp+1} &= S_{hp} + (\Lambda_h - \frac{(\beta_1 I_r + \beta_2 I_h)S_h}{N_h} - \mu_h S_h + \phi Q_h)h + \sigma_1 S_{hp}\Delta B_p + 0.5\sigma_1^2 S_{hp}\\
&((\Delta B_p)^2 - h),\\
E_{hp+1} &= E_{hp} + (\frac{(\beta_1 I_r + \beta_2 I_h)S_h}{N_h} - (\gamma_1 + \gamma_2 + \mu_h)E_h)h + \sigma_2 E_{hp}\Delta B_p + 0.5\sigma_2^2 E_{hp}\\
&((\Delta B_p)^2 - h),
\end{aligned}
$$

$$
\begin{aligned}
I_{hp+1} &= I_{hp} + (\gamma_1 E_h - (\mu_h + \delta_h + \rho) I_h)h + \sigma_3 I_{hp}\Delta B_p + 0.5\sigma_3^2 I_{hp}((\Delta B_p)^2 - h),\\
Q_{hp+1} &= Q_{hp} + (\gamma_2 E_h - (\phi + \tau + \mu_h + \delta_h) Q_h)h + \sigma_4 Q_{hp}\Delta B_p + 0.5\sigma_4^2 Q_{hp}((\Delta B_p)^2 - h),\\
R_{hp+1} &= R_{hp} + (\rho I_h + \tau Q_h - \mu_h R_h)h + \sigma_5 R_{hp}\Delta B_p + 0.5\sigma_5^2 R_{hp}((\Delta B_p)^2 - h)\\
S_{rp+1} &= S_{rp} + (\Lambda_r - \frac{\beta_3 S_r I_r}{N_r} - \mu_r S_r)h + \sigma_6 S_{rp}\Delta B_p + 0.5\sigma_6^2 S_{rp}((\Delta B_p)^2 - h),\\
E_{rp+1} &= E_{rp} + (\frac{\beta_3 S_r I_r}{N_r} - (\mu_r + \gamma_3) E_r)h + \sigma_7 E_{rp}\Delta B_p + 0.5\sigma_7^2 E_{rp}((\Delta B_p)^2 - h),\\
I_{rp+1} &= I_{rp} + (\gamma_3 E_r - (\mu_r + \delta_r) I_r)h + \sigma_8 I_{rp}\Delta B_p + 0.5\sigma_8^2 I_{rp}((\Delta B_p)^2 - h).
\end{aligned}
\tag{38}
$$

5.3. Numerical Scheme with Singular Kernel

To approximate the models (18)-(20). We will use GL-NSFDM [27] to solve (18) and (19). GL-NSFDM was selected for solving these system due to the following considerations:

- Consistency with fractional operators: The GL method provides a direct discretization of fractional derivatives and aligns well with the singular memory effects inherent in Caputo and Riemann-Liouville derivatives.
- Accuracy in long-term dynamics: Since monkeypox exhibits extended incubation and immunity effects, the GL method effectively captures the long-memory characteristics essential for modeling real-world epidemic data.
- Stability considerations: While the GL method is conditionally stable, we ensured numerical stability by selecting an appropriate step size h and confirming that the fractional-order system satisfied the necessary stability conditions.

Also, we use Milstein method (11) to approximate (20). For the stochastic version of the model, we employed the Milstein method to simulate the influence of random fluctuations in disease transmission. The key reasons for this choice include:

- Higher-order accuracy: Compared to the Euler-Maruyama method, the Milstein scheme incorporates additional correction terms that improve accuracy, which is crucial when modeling stochastic perturbations in disease dynamics.
- Stability in stochastic systems: Monkeypox outbreaks are subject to random environmental and demographic variations. The Milstein method provides better stability properties in capturing these fluctuations compared to lower-order stochastic solvers.
- Numerical Robustness: Given that stochastic differential equations (SDEs) can exhibit high sensitivity to parameter changes, the Milstein method's ability to handle noise-driven processes with higher precision ensures more reliable simulation results.

Consider the general form of variable order fractional Caputo differential equation as follows:

$$ {}_0^C D_t^{\kappa} Y(t) = f(t, Y(t)), \quad Y(0) = Y_0, \quad \kappa = \alpha(t) \in (0, 1]. \tag{39} $$

To approximate (39) using GL-NSFDM [27] as follows:

$$ f(t_p, Y_p) = \frac{1}{h^{\kappa}} (Y_{p+1} - \sum_{i=1}^{p+1} w_i Y_{p+1-i} - q_{p+1} Y_0). \tag{40} $$

By applying (40) for system (12) in $(0, t_1]$, the following is the explicit solution:

$$ \begin{aligned}
S_{hp+1} - \sum_{i=1}^{p+1} w_i S_{hp+1-i} - S_{h0} q_{p+1} &= h^{\kappa} (\Lambda_h^{\kappa} - \frac{(\beta_1^{\kappa} I_{rp} + \beta_2^{\kappa} I_{hp}) S_{hp+1}}{N_{hp}} \\
&\quad - \mu_h^{\kappa} S_{hp+1} + \phi^{\kappa} Q_{hp}), \\
E_{hp+1} - \sum_{i=1}^{p+1} w_i E_{hp+1-i} - q_{p+1} E_{h0} &= h^{\kappa} (\frac{(\beta_1^{\kappa} I_{rp} + \beta_2^{\kappa} I_{hp}) S_{hp+1}}{N_{hp}} \\
&\quad - (\gamma_1^{\kappa} + \gamma_2^{\kappa} + \mu_h^{\kappa}) E_{hp+1}), \\
I_{hp+1} - \sum_{i=1}^{p+1} w_i I_{hp+1-i} - q_{p+1} I_{h0} &= h^{\kappa} (\gamma_1^{\kappa} E_{hp+1} - (\mu_h^{\kappa} + \delta_h^{\kappa} + \rho^{\kappa}) I_{hp+1}), \\
Q_{hp+1} - \sum_{i=1}^{p+1} w_i Q_{hp+1-i} - q_{p+1} Q_{h0} &= h^{\kappa} (\gamma_2^{\kappa} E_{hp+1} - (\phi^{\kappa} + \tau^{\kappa} + \mu_h^{\kappa} + \delta_h^{\kappa}) Q_{hp+1}), \\
R_{hp+1} - \sum_{i=1}^{p+1} w_i R_{hp+1-i} - q_{p+1} R_{h0} &= h^{\kappa} (\rho^{\kappa} I_{hp+1} + \tau^{\kappa} Q_{hp+1} - \mu_h^{\kappa} R_{hp+1}), \\
S_{rp+1} - \sum_{i=1}^{p+1} w_i S_{rp+1-i} - q_{p+1} S_{r0} &= h^{\kappa} (\Lambda_r^{\kappa} - \frac{\beta_3^{\kappa} S_{rp+1} I_{rp}}{N_{rp}} - \mu_r^{\kappa} S_{rp+1}), \\
E_{rp+1} - \sum_{i=1}^{p+1} w_i E_{rp+1-i} - q_{p+1} E_{r0} &= h^{\kappa} (\frac{\beta_3^{\kappa} S_{rp+1} I_{rp}}{N_{rp}} - (\mu_r^{\kappa} + \gamma_3^{\kappa}) E_{rp+1}), \\
I_{rp+1} - \sum_{i=1}^{p+1} w_i I_{rp+1-i} - q_{p+1} I_{r0} &= h^{\kappa} (\gamma_3^{\kappa} E_{rp+1} - (\mu_r^{\kappa} + \delta_r^{\kappa}) I_{rp+1}).
\end{aligned} \tag{41} $$

The explicit expressions may be derived using a comprehensive fundamental calculation.

$$ \begin{aligned}
S_{hp+1} = \frac{1}{h^{\kappa} (\frac{(\beta_1^{\kappa} I_r + \beta_2^{\kappa} I_h)}{N_h} + \mu_h^{\kappa}) + 1} \Big[& h^{\kappa} (\Lambda_h^{\kappa} + \phi^{\kappa} Q_{hp+1}) \\
& + \sum_{i=1}^{p+1} w_i S_{hp+1-i} + q_{p+1} S_{h0} \Big],
\end{aligned} $$

$$
\begin{aligned}
E_{hp+1} &= \frac{1}{1+h^{\kappa}(\gamma_1^{\kappa}+\gamma_2^{\kappa}+\mu_h^{\kappa})}\left[\frac{\beta_1^{\kappa}I_{rp}+\beta_2^{\kappa}I_{hp})S_{hp+1}}{N_{hp}}\right.\\
&\left.+\sum_{i=1}^{p+1} w_i E_{hp+1-i}+q_{p+1}E_{h0}\right],\\
I_{hp+1} &= \frac{1}{1+h^{\kappa}(\mu_h^{\kappa}+\delta_h^{\kappa}+\rho^{\kappa})}\left[h^{\kappa}\gamma_1^{\kappa}E_{hp+1}+\sum_{i=1}^{p+1} w_i I_{hp+1-i}+q_{p+1}I_{h0}\right],\\
Q_{hp+1} &= \frac{1}{1+h^{\kappa}(\phi^{\kappa}+\tau^{\kappa}+\mu_h^{\kappa}+\delta_h^{\kappa})}\left[h^{\kappa}\gamma_2^{\kappa}E_{hp+1}\right.\\
&\left.+\sum_{i=1}^{p+1} w_i Q_{hp+1-i}+q_{p+1}Q_{h0}\right],\\
R_{hp+1} &= \frac{1}{1+h^{\kappa}\mu_h^{\kappa}}\left[h^{\kappa}(\rho^{\kappa}I_{hp+1}+\tau^{\kappa}Q_{hp+1})+\sum_{i=1}^{p+1} w_i R_{hp+1-i}+q_{p+1}R_{h0}\right],\\
S_{rp+1} &= \frac{1}{1+h^{\kappa}(\mu_r^{\kappa}+\frac{\beta_3^{\kappa}S_{rp+1}I_{rp}}{N_{rp}})}\left[h^{\kappa}\Lambda_r^{\kappa}+\sum_{i=1}^{p+1} w_i S_{rp+1-i}+q_{p+1}S_{r0}\right],\\
E_{rp+1} &= \frac{1}{1+h^{\kappa}(\mu_r^{\kappa}+\gamma_3^{\kappa})}\left[h^{\kappa}\frac{\beta_3^{\kappa}S_{rp+1}I_{rp}}{N_{rp}}+\sum_{i=1}^{p+1} w_i E_{rp+1-i}+q_{p+1}E_{r0}\right],\\
I_{rp+1} &= \frac{1}{1+h^{\kappa}(\mu_r^{\kappa}+\delta_r^{\kappa})}\left[h^{\kappa}\gamma_3^{\kappa}E_{rp+1}+\sum_{i=1}^{p+1} w_i I_{rp+1-i}+q_{p+1}I_{r0}\right].
\end{aligned}
\tag{42}
$$

Consider the general formula for fractal-fractional Caputo defferential equation in the $(t_1, t_2]$ given as follows:

$$
{}_0^{FFC}D_t^{\alpha,\beta}Y(t) = f(t, Y(t)), \qquad Y(0) = Y_0, \quad \alpha, \beta \in (0, 1]. \tag{43}
$$

Using the relation between fractal-fractional derivative and fractional order derivative [21] we have:

$$
t^{\beta-1}\beta f(t_p, Y_p) = \frac{1}{h^{\alpha}}(Y_{p+1} - \sum_{i=1}^{p+1} w_i Y_{p+1-i} - q_{p+1}Y_0). \tag{44}
$$

Applying the recommended numerical approach (44) to approximate the system (19) yields the following results:

$$
\begin{aligned}
\frac{1}{h^{\alpha}}(S_{hp+1} - \sum_{i=1}^{p+1} w_i S_{hp+1-i} - q_{p+1}S_{h0}) = (\beta t^{\beta-1})\left[\Lambda_h^{\alpha} - \frac{(\beta_1^{\alpha}I_{rp}+\beta_2^{\alpha}I_{hp})S_{hp+1}}{N_{hp}}\right.\\
\left.-\mu_h^{\alpha}S_{hp+1}+\phi^{\alpha}Q_{hp}\right],
\end{aligned}
$$

$$\frac{1}{h^\alpha}(E_{hp+1}-\sum_{i=1}^{p+1}w_iE_{hp+1-i}-q_{p+1}E_{h0})=(\beta t^{\beta-1})\left[\frac{(\beta_1^\alpha I_{rp}+\beta_2^\alpha I_{hp})S_{hp+1}}{N_{hp}}\right.$$
$$\left.-(\gamma_1^\alpha+\gamma_2^\alpha+\mu_h^\alpha)E_{hp+1}\right],$$
$$\frac{1}{h^\alpha}(I_{hp+1}-\sum_{i=1}^{p+1}w_iI_{hp-i+1}-I_{h0}q_{p+1})=(\beta t^{\beta-1})(\gamma_1^\alpha E_{hp+1}-(\mu_h^\alpha+\delta_h^\alpha+\rho^\alpha)I_{hp+1}),$$
$$\frac{1}{h^\alpha}(Q_{hp+1}-\sum_{i=1}^{p+1}w_iQ_{hp-i+1}-Q_{h0}q_{p+1})=(\beta t^{\beta-1})(\gamma_2^\alpha E_{hp+1}-(\phi^\alpha+\tau^\alpha+\mu_h^\alpha+\delta_h^\alpha)Q_{hp+1}),$$
$$\frac{1}{h^\alpha}(R_{hp+1}-\sum_{i=1}^{p+1}w_iR_{hp-i+1}-R_{h0}q_{p+1})=(\beta t^{\beta-1})(\rho^\alpha I_{hp+1}+\tau^\alpha Q_{hp+1}-\mu_h^\alpha R_{hp+1}),$$
$$\frac{1}{h^\alpha}(S_{rp+1}-\sum_{i=1}^{p+1}w_iS_{rp-i+1}-S_{r0}q_{p+1})=(\beta t^{\beta-1})(\Lambda_r^\alpha-\frac{\beta_3^\alpha S_{rp+1}I_{rp}}{N_{rp}}-\mu_r^\alpha S_{rp+1}),$$
$$\frac{1}{h^\alpha}(E_{rp+1}-\sum_{i=1}^{p+1}w_iE_{rp-i+1}-E_{r0}q_{p+1})=(\beta t^{\beta-1})(\frac{\beta_3^\alpha S_{rp+1}I_{rp}}{N_{rp}}-(\mu_r^\alpha+\gamma_3^\alpha)E_{rp+1}),$$
$$\frac{1}{h^\alpha}(I_{rp+1}-\sum_{i=1}^{p+1}w_iI_{rp-i+1}-I_{r0}q_{p+1})=(\beta t^{\beta-1})(\gamma_3^\alpha E_{rp+1}-(\mu_r^\alpha+\delta_r^\alpha)I_{rp+1}). \tag{45}$$

302 To obtain the explicit expressions, a comprehensive calculation can be carried out.

$$S_{hp+1}=\frac{1}{1+\beta t^{\beta-1}h^\alpha(\frac{(\beta_1^\alpha I_r+\beta_2^\alpha I_h)}{N_h}+\mu_h^\alpha)}\left[\beta t^{\beta-1}h^\alpha(\Lambda_h^\alpha+\phi^\alpha Q_{hp+1})\right.$$
$$\left.+\sum_{i=1}^{p+1}w_iS_{hp+1-i}+q_{p+1}S_{h0}\right],$$
$$E_{hp+1}=\frac{1}{1+\beta t^{\beta-1}h^\alpha(\gamma_1^\alpha+\gamma_2^\alpha+\mu_h^\alpha)}\left[\beta t^{\beta-1}h^\alpha\frac{(\beta_1^\alpha I_{rp}+\beta_2^\alpha I_{hp})S_{hp+1}}{N_{hp}}\right.$$
$$\left.+\sum_{i=1}^{p+1}w_iE_{hp+1-i}+q_{p+1}E_{h0}\right],$$
$$I_{hp+1}=\frac{1}{1+\beta t^{\beta-1}h^\alpha(\mu_h^\alpha+\delta_h^\alpha+\rho^\alpha)}\left[\beta t^{\beta-1}h^\alpha\gamma_1^\alpha E_{hp+1}+\sum_{i=1}^{p+1}w_iI_{hp+1-i}+q_{p+1}I_{h0}\right],$$
$$Q_{hp+1}=\frac{1}{1+\beta t^{\beta-1}h^\alpha(\phi^\alpha+\tau^\alpha+\mu_h^\alpha+\delta_h^\alpha)}\left[\beta t^{\beta-1}h^\alpha\gamma_2^\alpha E_{hp+1}\right.$$
$$\left.+\sum_{i=1}^{p+1}w_iQ_{hp+1-i}+q_{p+1}Q_{h0}\right],$$

$$
\begin{aligned}
R_{hp+1} &= \frac{1}{1+\beta t^{\beta-1}h^{\alpha}\mu_h^{\alpha}}\left[\beta t^{\beta-1}h^{\alpha}(\rho^{\alpha}I_{hp+1}+\tau^{\alpha}Q_{hp+1})+\sum_{i=1}^{p+1}w_i R_{hp+1-i}+q_{p+1}R_{h0}\right],\\
S_{rp+1} &= \frac{1}{1+\beta t^{\beta-1}h^{\alpha}(\mu_r^{\alpha}+\frac{\beta_3^{\alpha}S_{rp+1}I_{rp}}{N_{rp}})}\left[\beta t^{\beta-1}h^{\alpha}\Lambda_r^{\alpha}+\sum_{i=1}^{p+1}w_i S_{rp+1-i}+q_{p+1}S_{r0}\right],\\
E_{rp+1} &= \frac{1}{1+\beta t^{\beta-1}h^{\alpha}(\mu_r^{\alpha}+\gamma_3^{\alpha})}\left[\beta t^{\beta-1}h^{\alpha}\frac{\beta_3^{\alpha}S_{rp+1}I_{rp}}{N_{rp}}+\sum_{i=1}^{p+1}w_i E_{rp+1-i}+q_{p+1}E_{r0}\right],\\
I_{rp+1} &= \frac{1}{1+\beta t^{\beta-1}h^{\alpha}(\mu_r^{\alpha}+\delta_r^{\alpha})}\left[\beta t^{\beta-1}h^{\alpha}\gamma_3^{\alpha}E_{rp+1}+\sum_{i=1}^{p+1}w_i I_{rp+1-i}+q_{p+1}I_{r0}\right].
\end{aligned}
\tag{46}
$$

In the third interval $(t_2, T_f])$, to approximate the system (20), we will use Milstein method (11). Then the explicit solution given as follows:

$$
\begin{aligned}
S_{hp+1} &= S_{hp}+(\Lambda_h-\frac{(\beta_1 I_r+\beta_2 I_h)S_h}{N_h}-\mu_h S_h+\phi Q_h)h+\sigma_1 S_{hp}\Delta B_p+0.5\sigma_1^2 S_{hp}\\
&\quad((\Delta B_p)^2-h),\\
E_{hp+1} &= E_{hp}+(\frac{(\beta_1 I_r+\beta_2 I_h)S_h}{N_h}-(\gamma_1+\gamma_2+\mu_h)E_h)h+\sigma_2 E_{hp}\Delta B_p+0.5\sigma_2^2 E_{hp}\\
&\quad((\Delta B_p)^2-h),\\
I_{hp+1} &= I_{hp}+(\gamma_1 E_h-(\mu_h+\delta_h+\rho)I_h)h+\sigma_3 I_{hp}\Delta B_p+0.5\sigma_3^2 I_{hp}((\Delta B_p)^2-h),\\
Q_{hp+1} &= Q_{hp}+(\gamma_2 E_h-(\phi+\tau+\mu_h+\delta_h)Q_h)h+\sigma_4 Q_{hp}\Delta B_p+0.5\sigma_4^2 Q_{hp}((\Delta B_p)^2-h),\\
R_{hp+1} &= R_{hp}+(\rho I_h+\tau Q_h-\mu_h R_h)h+\sigma_5 R_{hp}\Delta B_p+0.5\sigma_5^2 R_{hp}((\Delta B_p)^2-h),\\
S_{rp+1} &= S_{rp}+(\Lambda_r-\frac{\beta_3 S_r I_r}{N_r}-\mu_r S_r)h+\sigma_6 S_{rp}\Delta B_p+0.5\sigma_6^2 S_{rp}((\Delta B_p)^2-h),\\
E_{rp+1} &= E_{rp}+(\frac{\beta_3 S_r I_r}{N_r}-(\mu_r+\gamma_3)E_r)h+\sigma_7 E_{rp}\Delta B_p+0.5\sigma_7^2 E_{rp}((\Delta B_p)^2-h),\\
I_{rp+1} &= I_{rp}+(\gamma_3 E_r-(\mu_r+\delta_r)I_r)h+\sigma_8 I_{rp}\Delta B_p+0.5\sigma_8^2 I_{rp}((\Delta B_p)^2-h).
\end{aligned}
\tag{47}
$$

Remark 5.3. *Regarding the stability for this method, you can find it in [27].*

6. Numerical Simulations

This part aims to verify the provided experimental results as well as the analytical expressions that were produced in the preceding sections. From t=0 on June 13 to t=95 on September 16, using the infected cases, 2022 (96 data points) [25]. $S_{h0}=10000, E_{h0}=50, I_{h0}=5.86, Q_{h0}=1.14, R_{h0}=0, S_{r0}=1000, E_{r0}=100$, and $I_{r0}=10$ are the model's

starting values. Table 2 lists the values of this model's parameters.
Multiple behaviours are displayed by the dynamics.This enables us to analyse and predict how the disease will develop from the beginning to the end, giving us the chance to see a variety of behaviours from crossover to stochastic processes. We got the results of infection cases from utilizing the techniques (27)-(31), (34)-(38), and (42)-(47) for the provided crossover models (12)-(14), (15)-(17), and (18)-(20), which are compared with real-life information from the United States (June 13, 2022, to September 16, 2022). Figures 1-4 show the numerical results of the first crossover (12)-(14) model with non-singular kernel with different values of α, β, and κ. In Figures 1-2, we contrasted real data with the outcomes of infected humans that were produced using the suggested model (12)-(14). We noted the good results we have at $\alpha = 0.97, 0.99, \beta = 0.99$, and $\kappa = 0.98 - 0.001sin(t/10)^2$, and $\alpha = 0.93, 0.97, \beta = 0.99$, and $\kappa = 0.98 - 0.001cos(t/50)$. Figure 3 describes the effect of changing α in behavior of the solution. Also, Figure 4 shows the solution behavior for the considered model at different values of α, β and $\kappa = 0.94 - 0.01t$.

Figures 5-8 show the numerical results of the first crossover (15)-(17) model with non-singular kernel and distinct α, β, and κ values. Also, we observed from Figures 7-8, the good results appear when $\alpha = 0.93, 0.97, \beta = 0.99$, and $\kappa = 0.98 - 0.001sin(t/10)^2$, and $\alpha = 0.93, \beta = 0.99$, with $\kappa = 0.95 - 0.001cos(t/50)$.

Figures 9-12 show the numerical results of the first crossover (18)-(20) model with singular kernel and different values of α, β, and κ. Also, we noted that from Figures 11-12, the good results appear when $\alpha = 0.93, 0.95, \beta = 0.99$, and $\kappa = 0.98 - 0.001sin(t/10)^2$.

Table 3 shows the CPU time for three schemes (27)-(31), (34)-(38), and (42)-(47), we noted that the scheme (34)-(38) with singular kernel is the fastest one.

We concluded that from the comparesion with real data the best result we have from the first crossover model (14)-(12) with a non-singular kernel. Moreover if we compare our result with [28], we have excellent results.

Table 3: The CPU time at $T_f = 100, \alpha = 0.95, \beta = 0.99, \kappa = 0.94 - 0.01t$.

h	CM1	CM2	CM3
1			0.0348147
0.2	0.8495	0.155779	0.1417802
0.1	3.3487	0.549053	0.2576076
0.06	7.5111	1.085631	0.408594

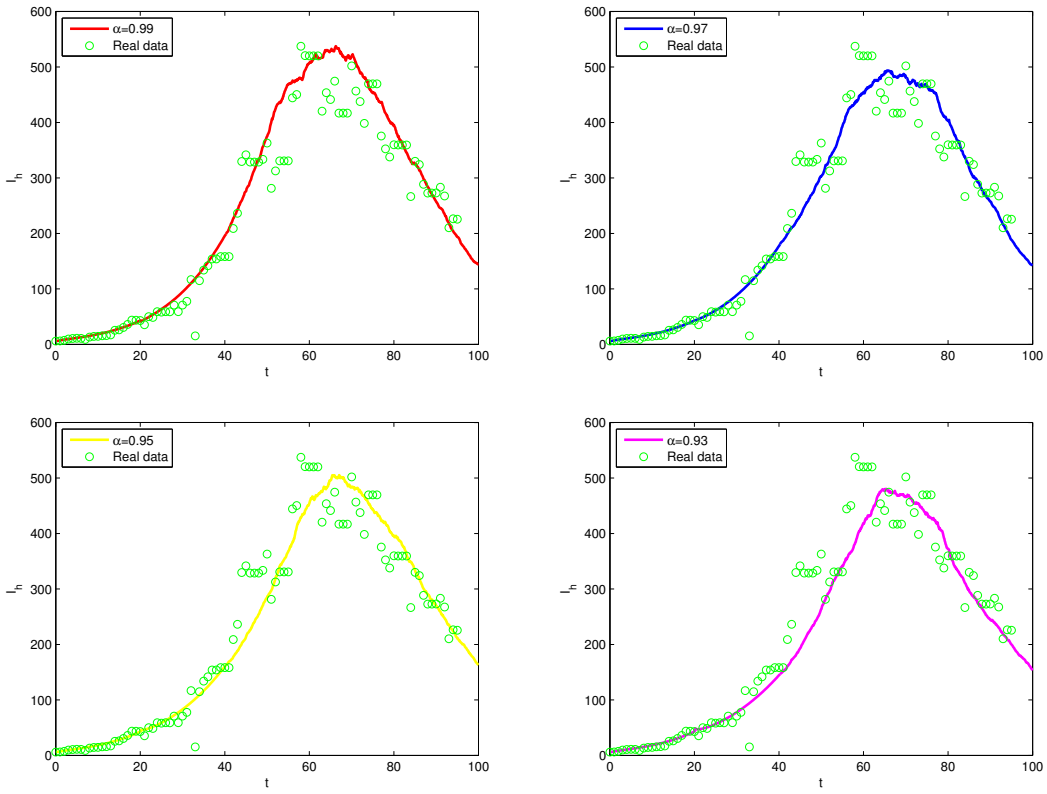

Figure 1: Numerical simulation of the piecewise system (12)-(14) at various α, $\beta = 0.99$ and $\kappa = 0.98 - 0.001sin^2(t/10)$

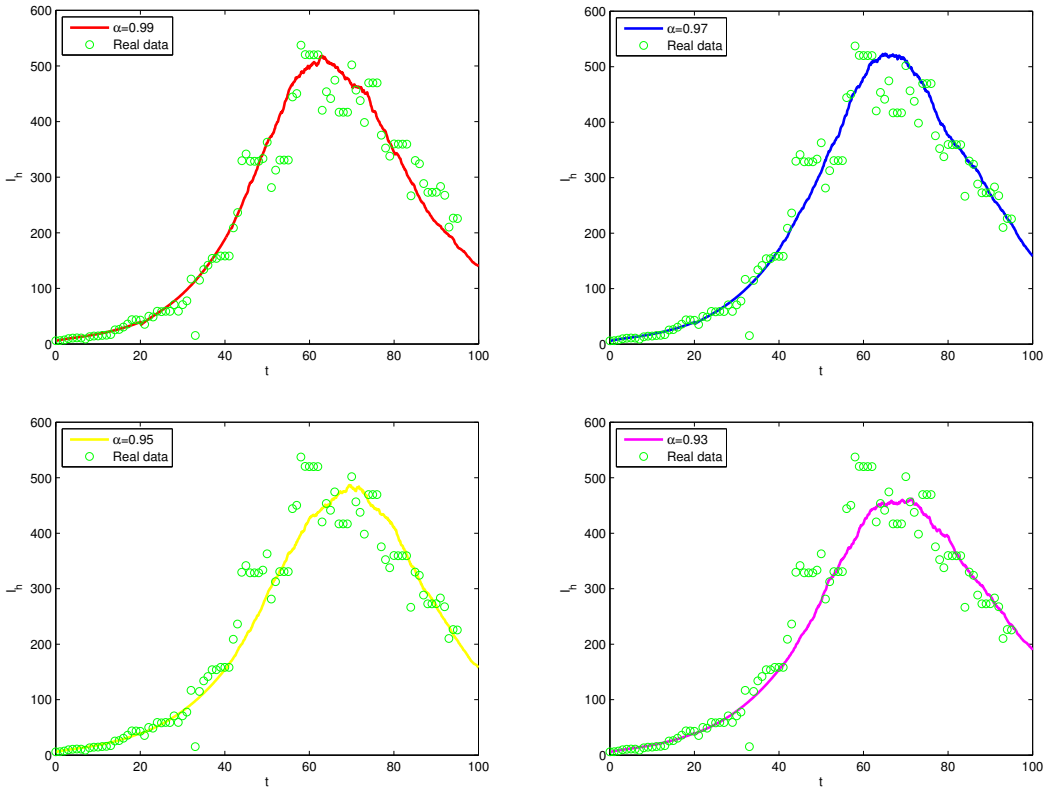

Figure 2: Numerical simulation of the piecewise system (12)-(14) at various α, $\beta = 0.99$ and $\kappa = 0.95 - 0.001cos(t/50)$

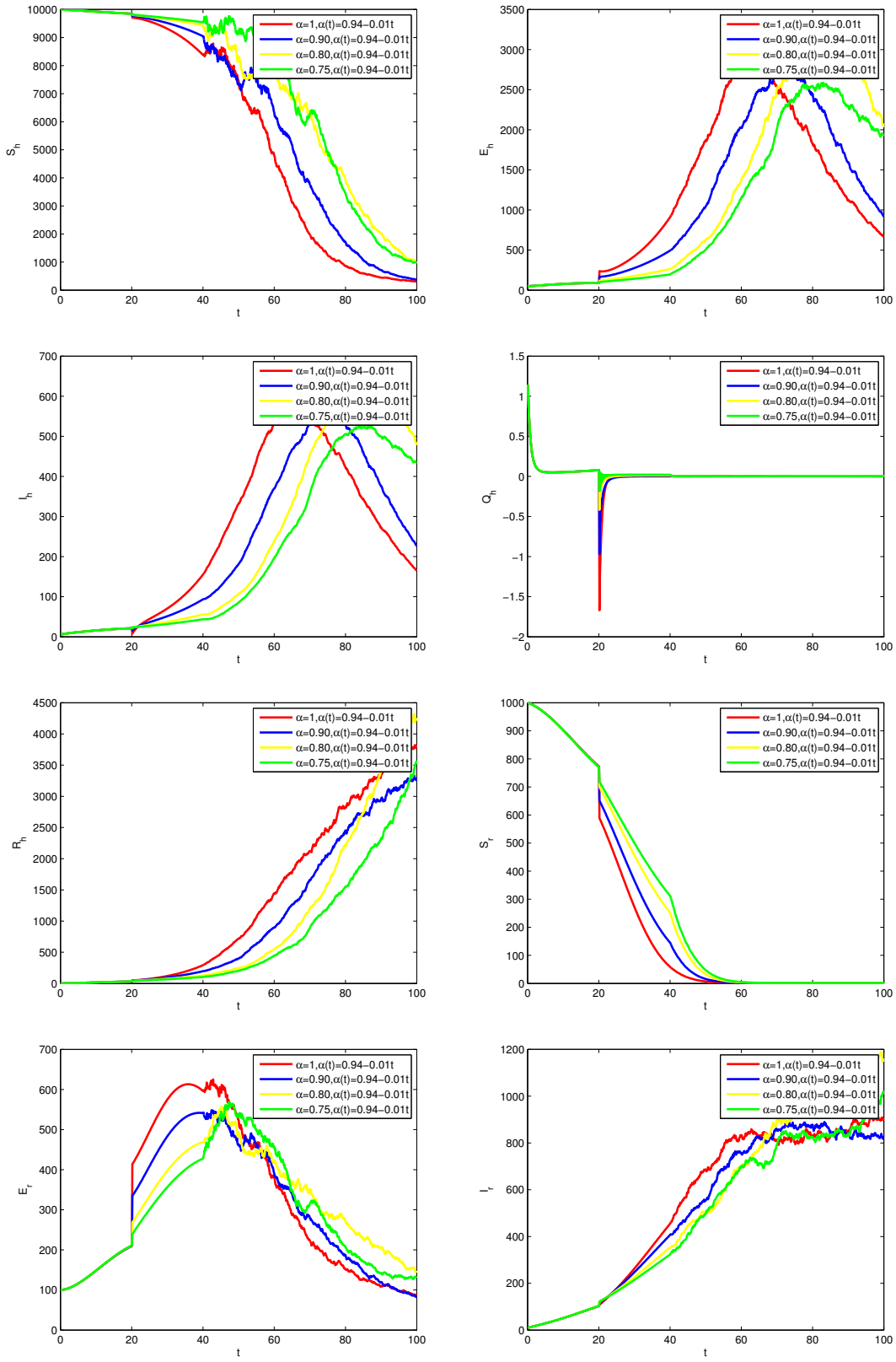

Figure 3: Numerical simulation of the piecewise system (12)-(14) at various values α , β=0.99, κ=0.94-0.01t, σ_1=0.01, σ_2 = 0.05, = 0.02, σ_3= 0.01, σ_4 = 0.05, σ_5 = 0.02, σ_6 = 0.01, σ_7 = 0.05 and σ_8 = 0.02

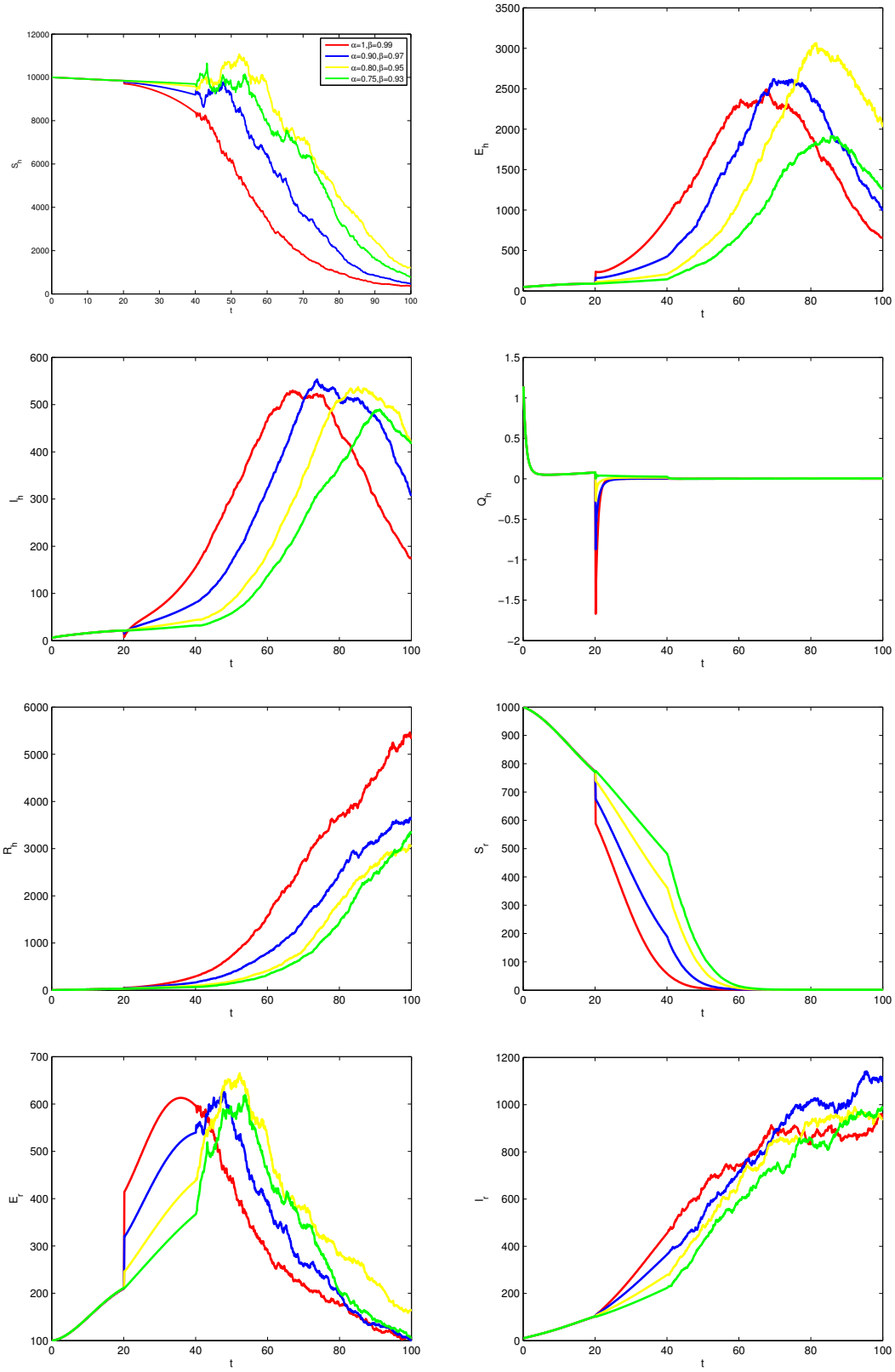

Figure 4: Numerical simulation of the piecewise system (12)-(14) at various values α , β, κ=0.94-0.01t, $\sigma_1 = 0.01$, $\sigma_2 = 0.05$, = 0.02, σ_3= 0.01, $\sigma_4 = 0.05$, $\sigma_5 = 0.02$, $\sigma_6 = 0.01$, $\sigma_7 = 0.05$ and $\sigma_8 = 0.02$

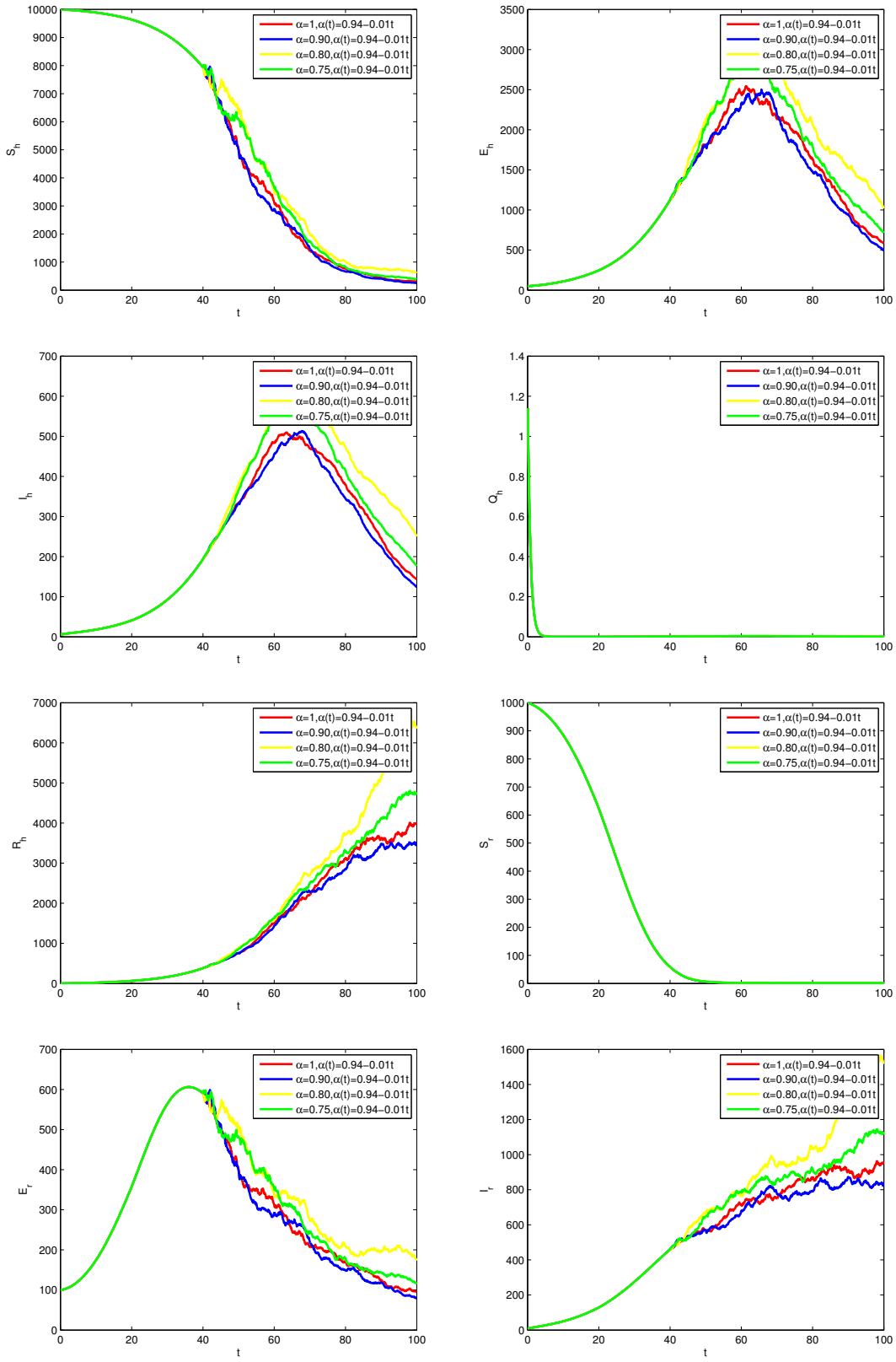

Figure 5: Numerical simulation of the piecewise system (15)-(17) at various values α , β=0.99, κ=0.94-0.01t, σ_1=0.01, σ_2 = 0.05, = 0.02, σ_3= 0.01, σ_4 = 0.05, σ_5 = 0.02, σ_6 = 0.01, σ_7 = 0.05 and σ_8 = 0.02

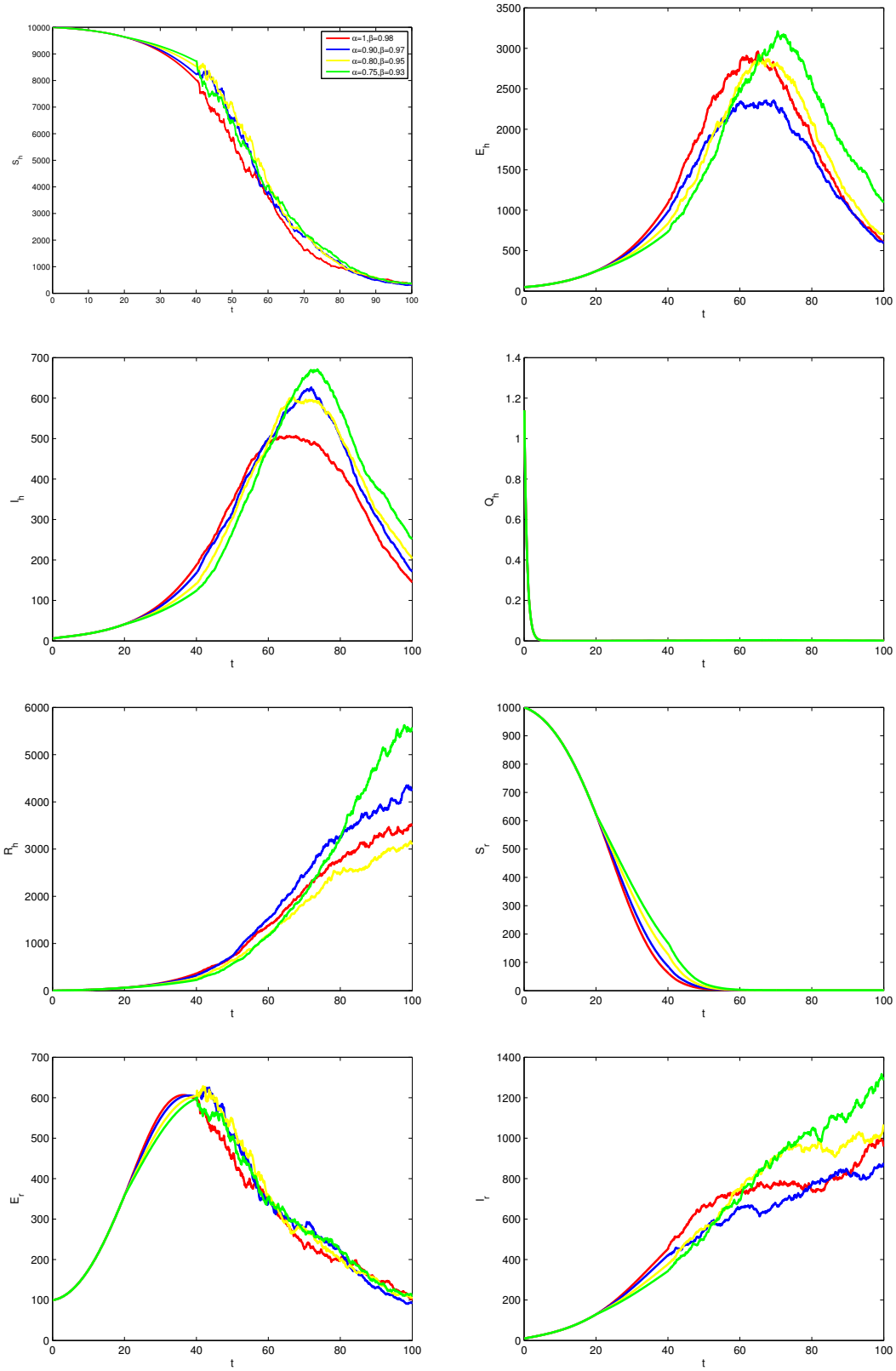

Figure 6: Numerical simulation of the piecewise system (15)-(17) at various values α , β, κ=0.94-0.01t, $\sigma_1 = 0.01$, $\sigma_2 = 0.05$, = 0.02, σ_3= 0.01, $\sigma_4 = 0.05$, $\sigma_5 = 0.02$, $\sigma_6 = 0.01$, $\sigma_7 = 0.05$ and $\sigma_8 = 0.02$

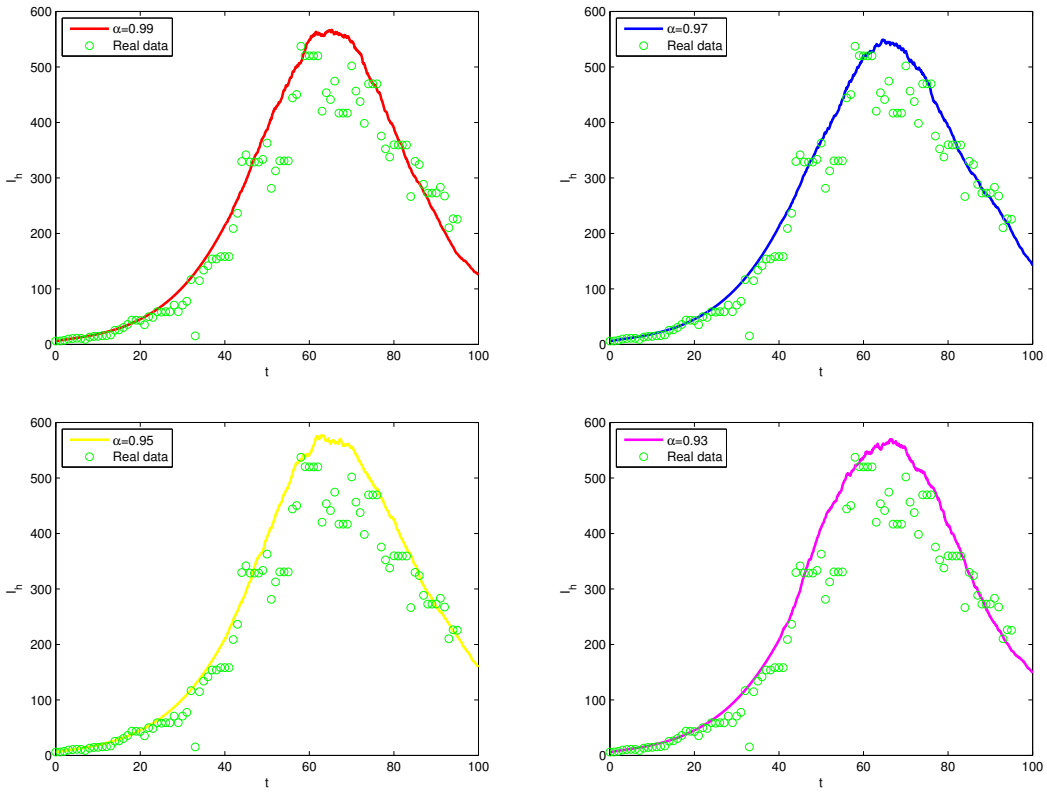

Figure 7: Numerical simulation of the piecewise system (15)-(17) numerical simulation at various α, $\beta = 0.99$ and $\kappa = 0.98 - 0.001sin^2(t/10)$

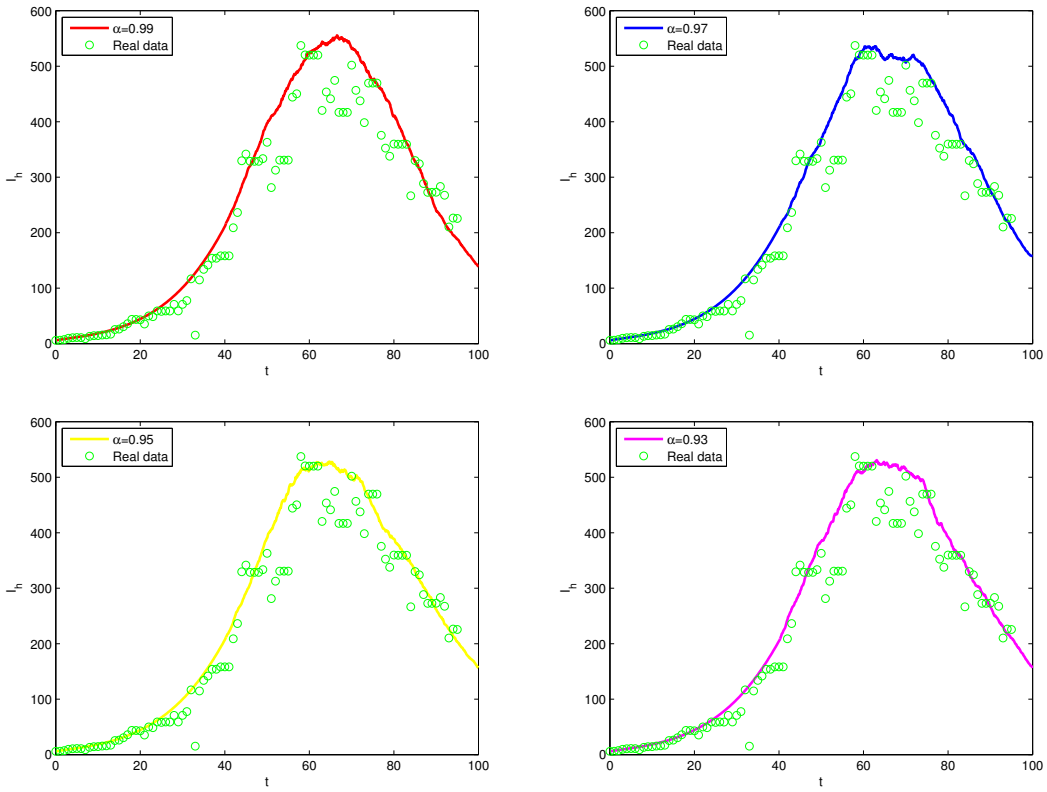

Figure 8: Numerical simulation of the piecewise system (15)-(17) at various values α, $\beta = 0.99$ and $\kappa = 0.95 - 0.001cos(t/50)$

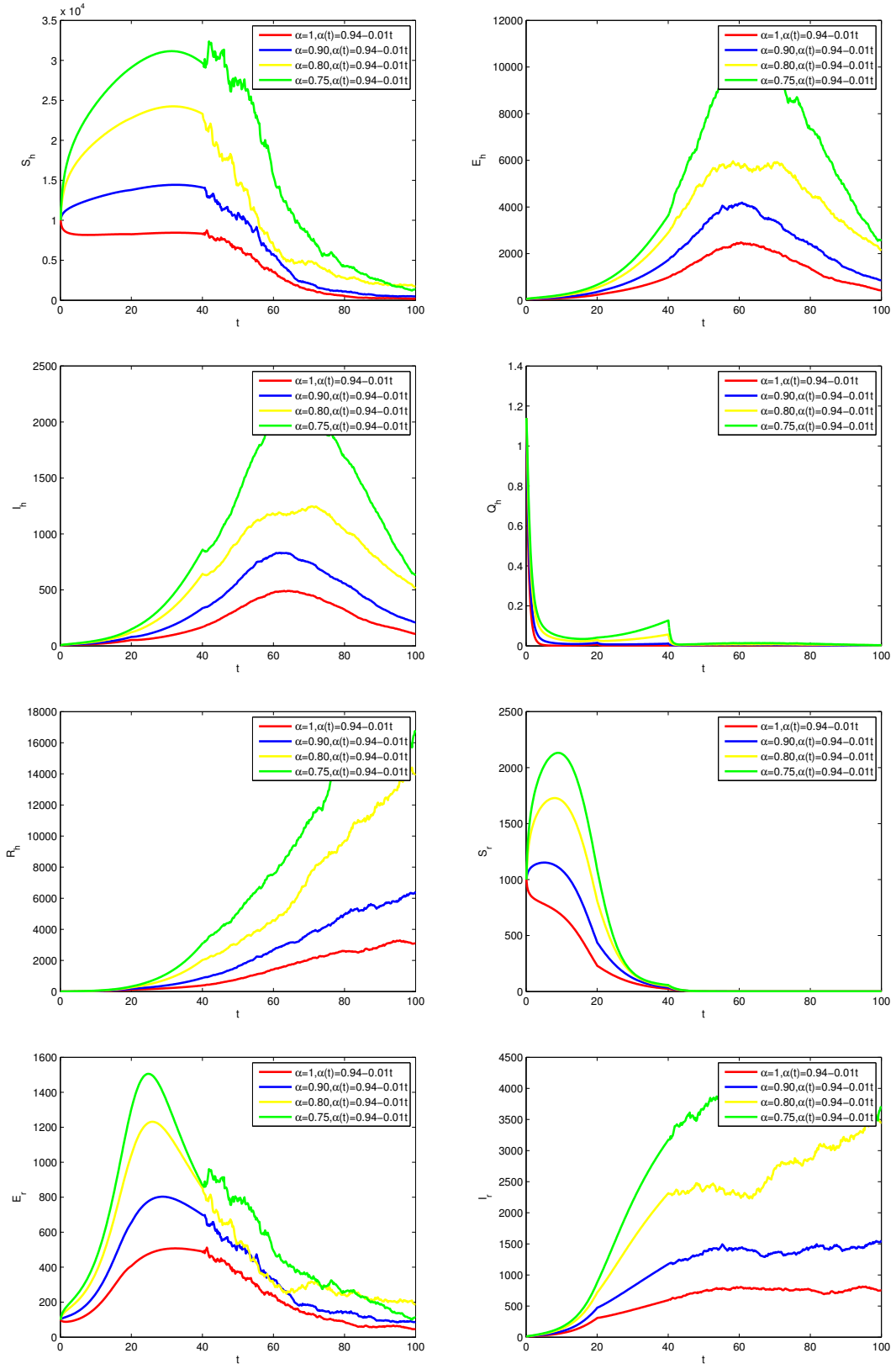

Figure 9: Numerical simulation of the piecewise system (18)-(20) at various values α , β=0.99, κ=0.94-0.01t, σ_1=0.01, σ_2 = 0.05, = 0.02, σ_3= 0.01, σ_4 = 0.05, σ_5 = 0.02, σ_6 = 0.01, σ_7 = 0.05 and σ_8 = 0.02

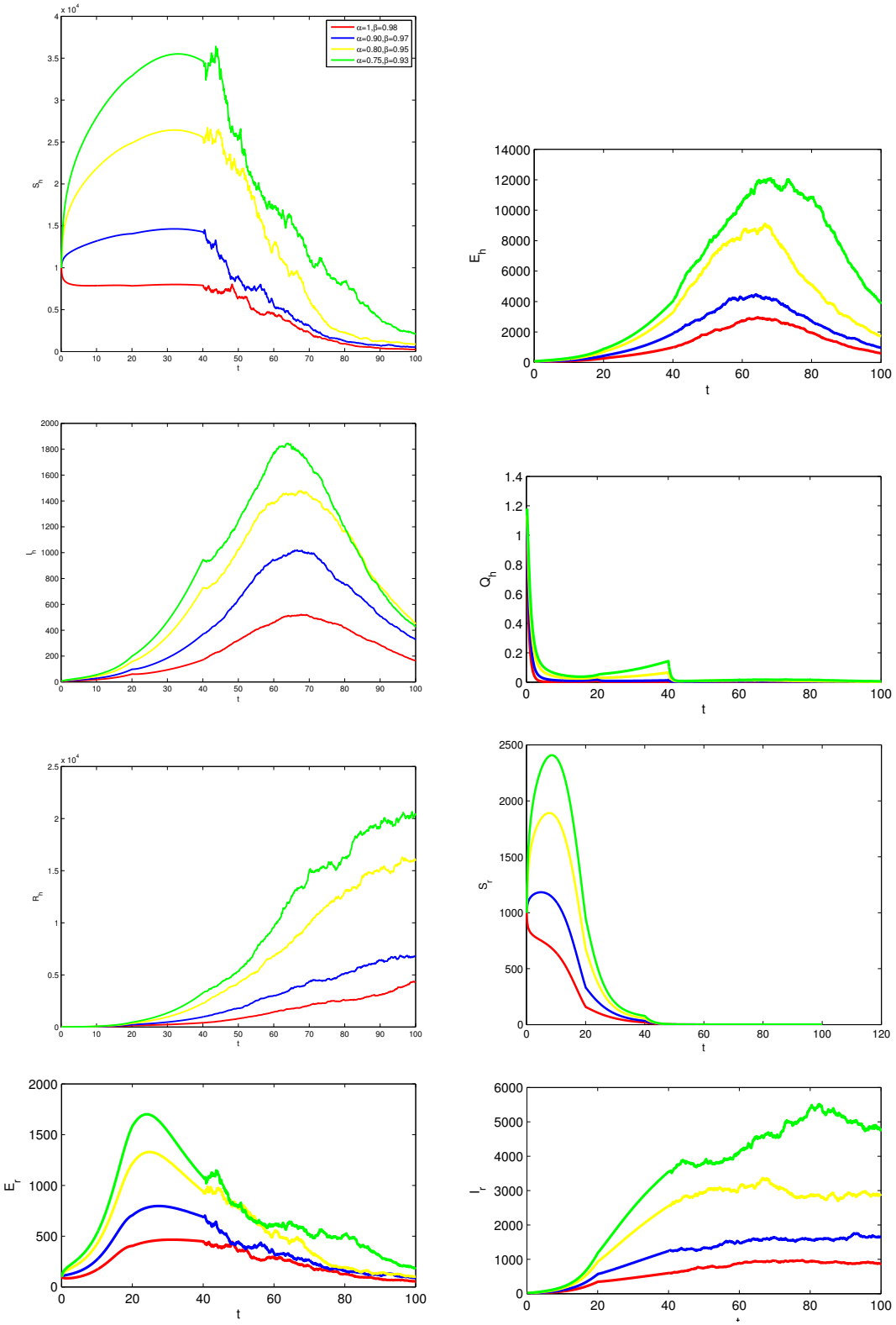

Figure 10: Numerical simulation of the piecewise system (18)-(20) at various values α , β, κ=0.94-0.01t, $\sigma_1 = 0.01$, $\sigma_2 = 0.05$, = 0.02, σ_3= 0.01, $\sigma_4 = 0.05$, $\sigma_5 = 0.02$, $\sigma_6 = 0.01$, $\sigma_7 = 0.05$ and $\sigma_8 = 0.02$

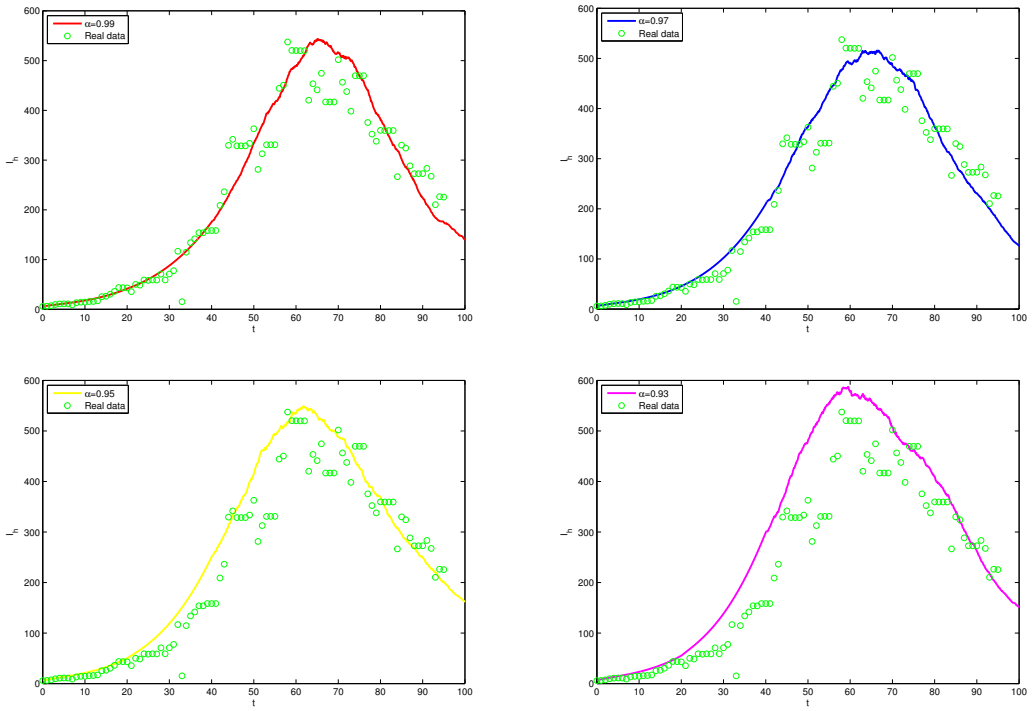

Figure 11: Numerical simulation of the piecewise system (18)-(20) at various values α, $\beta = 0.99$ and $\kappa = 0.98 - 0.001sin^2(t/10)$

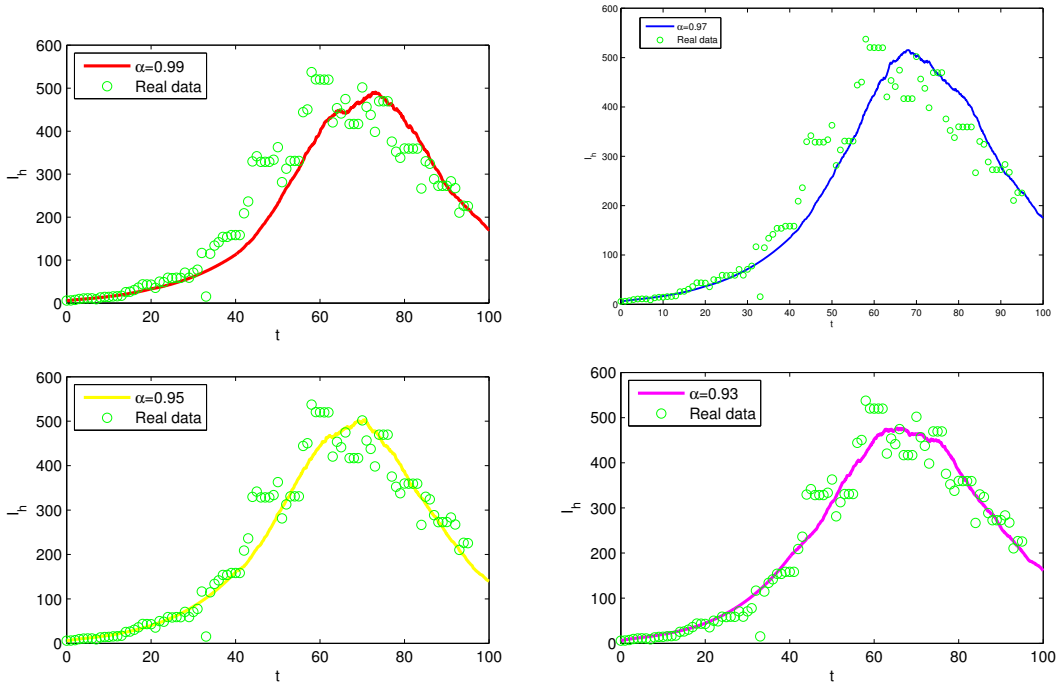

Figure 12: Numerical simulation of the piecewise system (18)-(20) at various values α, $\beta = 0.99$ and $\kappa = 0.95 - 0.001cos(t/50)$

7. Conclusions

This study presents three crossover models on Monkeypox disease which combine Caputo, Mittag-Leffler, and the Caputo-Fabrizio definitions. A combination of three models variable order fractional, fractal-fractional, and stochastic with their piecewise derivatives to describe a Monkypox disease are presented in three intervals of time. The nonstandard Grünwald−Letnikov finite difference method was used to approximate the deterministic models with a singular kernel and the Toufik-Atangana technique to approximate the deterministic model involves a nonsingular Mittag-Leffler kernel. Moreover, the approximation of the integral Caputo-Fabrizio and Lagrange polynomials of two steps was used to approximate the deterministic model with a nonsingular exponential decay kernel. The Milstein method was implemented to approximate the stochastic differential equation. Analysis was done on the suggested model's stability.
Regarding the impact of these kernels on model outcomes:

- Singular kernels (e.g., Caputo fractional derivative) introduce power-law memory effects, meaning past states significantly influence present disease dynamics. This results in a slower decay of past influences, prolonged epidemic waves, and stronger hysteresis effects in the system. As a consequence, the disease dynamics exhibit a more persistent infection tail and slower stabilization.

- Non-singular kernels (e.g., Atangana-Baleanu and Caputo-Fabrizio fractional derivatives) employ exponentially decaying memory effects, where the impact of past states diminishes more rapidly. This leads to faster stabilization of the disease, shorter memory retention, and more immediate responses to changes in transmission dynamics.

From the numerical comparison between these three operators, we found that CM1 is the fastest one. Also, the GL-NSFDM is more efficient than others because it can work with big step sizes. Moreover, from comparison the results of three crossover model with real data, we found that the first crossover model with non singular kernel and ABC operator is the best one to describe the monkeybox model.

The piecewise crossover differential equations, constructed with fractional and variable order operators alongside stochastic derivatives, have opened new avenues for researchers across various fields, enabling them to capture diverse behaviors over time intervals. Applying this approach to real-world problems allow researchers to more accurately reflect reality.

References

[1] Centers for Disease Control and Prevention. U.S. Monkeypox case trends reported to CDC. https://www.cdc.gov/poxvirus/monkeypox/response/2022/mpx-trends.html, 2022.

[2] A. A. Aljabali, M. A. Obeid, M. B. Nusair, A. Hmedat, and M. M. Tambuwala. Monkeypox virus: an emerging epidemic. *Microbial Pathogenesis*, 173(Pt A):105794, 2022.

[3] J. G. Breman. Monkeypox: an emerging infection for humans. In *Emerging Viruses in Human Populations*, pages 45–67. John Wiley & Sons, Ltd, Chichester, 2000.

[4] R. S. Levine, A. T. Peterson, K. L. Yorita, D. Carroll, I. K. Damon, and M. G. Reynolds. Ecological niche and geographic distribution of human monkeypox in Africa. *PLoS ONE*, 2(1):e176, 2007.

[5] S. Usman and I. Isa Adamu. Modeling the transmission dynamics of the monkeypox virus infection with treatment and vaccination interventions. *Journal of Applied Mathematics and Physics*, 5(12):2335–2353, 2017.

[6] A. Khan, Y. Sabbar, and A. Din. Stochastic modeling of the Monkeypox 2022 epidemic with cross-infection hypothesis in a highly disturbed environment. *Mathematical Biosciences and Engineering*, 19(12):13560–13581, 2022.

[7] R. Grant, L.-L. Nguyen, and R. Breban. Modelling human-to-human transmission of monkeypox. *Bulletin of the World Health Organization*, 98(9):638–640, 2020.

[8] S. V. Bankuru, S. Kossol, W. Hou, P. Mahmoudi, J. Rychtář, and D. Taylor. A game-theoretic model of Monkeypox to assess vaccination strategies. *PeerJ*, 8:e9272, 2020.

[9] N. H. Sweilam, S. M. AL-Mekhlafi, and A. Almutairi. Fractal fractional optimal control for a novel malaria mathematical model; a numerical approach. *Results in Physics*, 19:103446, 2020.

[10] M. Y. Sahnoune, A. Ez-zetouni, K. Akdim, et al. Qualitative analysis of a fractional-order two-strain epidemic model with vaccination and general non-monotonic incidence rate. *International Journal of Dynamics and Control*, 11(4):1532–1543, 2023.

[11] C. Xu, C. Aouiti, M. Liao, P. Li, and Z. Liu. Chaos control strategy for a fractional-order financial model. *Advances in Difference Equations*, 2020:573, 2020.

[12] K. N. Nabi, H. Abboubakar, and P. Kumar. Forecasting of COVID-19 pandemic: from integer derivatives to fractional derivatives. *Chaos, Solitons & Fractals*, 141:110283, 2020.

[13] S. K. Biswas, U. Ghosh, and S. Sarkar. Mathematical model of Zika virus dynamics with vector control and sensitivity analysis. *Infectious Disease Modelling*, 5:23–41, 2020.

[14] S. Hasan, A. El-Ajou, S. Hadid, M. Al-Smadi, and S. Momani. Atangana-Baleanu fractional framework of reproducing kernel technique in solving fractional population dynamics system. *Chaos, Solitons & Fractals*, 133:109624, 2020.

[15] R. P. Chauhan, S. Kumar, B. S. T. Alkahtani, and S. S. Alzaid. A study on fractional order financial model by using Caputo-Fabrizio derivative. *Results in Physics*, 57:107335, 2024.

[16] N. H. Sweilam, F. A. Rihan, and S. M. AL-Mekhlafi. A fractional-order delay differential model with optimal control for cancer treatment based on synergy between anti-angiogenic and immune cell therapies. *Discrete and Continuous Dynamical Systems - Series S*, 13(9):2403–2424, 2020.

[17] J. Danane, Z. Hammouch, K. Allali, S. Rashid, and J. Singh. A fractional-order model of coronavirus disease 2019 (COVID-19) with governmental action and individual reaction. *Mathematical Methods in the Applied Sciences*, 46(7):7808–7824, 2023.

[18] M. Zamir, F. Nadeem, T. Abdeljawad, and Z. Hammouch. A fractional multi-order model to predict the COVID-19 outbreak in Morocco. *Applied and Computational Mathematics*, 20(1):177–203, 2021.

[19] K. Shah, T. Abdeljawad, and A. Ali. Mathematical analysis of the Cauchy type dynamical system under piecewise equations with Caputo fractional derivative. *Chaos, Solitons & Fractals*, 161:112356, 2022.

[20] X. P. Li, H. F. Alrihieli, E. A. Algehyne, M. A. Khan, M. Y. Alshahrani, Y. Alraey, and M. B. Riaz. Application of piecewise fractional differential equation to COVID-19 infection dynamics. *Results in Physics*, 39:105685, 2022.

[21] A. Atangana and S. İğret Araz. *New Numerical Scheme with Newton Polynomial: Theory, Methods, and Applications*. Academic Press, London, 2021.

[22] S. Etemad, I. Avci, P. Kumar, D. Baleanu, and S. Rezapour. Some novel mathematical analysis on the fractal–fractional model of the AH1N1/09 virus and its generalized Caputo-type version. *Chaos, Solitons & Fractals*, 162:112511, 2022.

[23] P. E. Kloeden and E. Platen. *Numerical Solution of Stochastic Differential Equations*, volume 23 of *Stochastic Modelling and Applied Probability*. Springer, Berlin, 1992.

[24] G. N. Mil'shtejn. Approximate integration of stochastic differential equations. *Theory of Probability and Its Applications*, 19(3):557–562, 1975.

[25] O. J. Peter, S. Kumar, N. Kumari, et al. Transmission dynamics of Monkeypox virus: a mathematical modelling approach. *Modeling Earth Systems and Environment*, 8(3):3423–3434, 2022.

[26] O. J. Peter, S. Kumar, N. Kumari, F. A. Oguntolu, K. Oshinubi, and R. Musa. Transmission dynamics of Monkeypox virus: a mathematical modelling approach. *Modeling Earth Systems and Environment*, 8(3):3423–3434, 2022.

[27] A. J. Arenas, G. González-Parra, and B. M. Chen-Charpentier. Construction of nonstandard finite difference schemes for the SI and SIR epidemic models of fractional order. *Mathematics and Computers in Simulation*, 121:48–63, 2016.

[28] P. Kumar, M. Vellappandi, Z. Khan, S. M. Sivalingam, A. Kaziboni, and V. Govindaraj. A case study of monkeypox disease in the United States using mathematical modeling with real data. *Mathematics and Computers in Simulation*, 213:444–465, 2023.